Post-Newtonian accurate parametric solution to the dynamics of spinning compact binaries in eccentric orbits: The leading order spin-orbit interaction

Christian Königsdörffer* and Achamveedu Gopakumar†

Theoretisch-Physikalisches Institut, Friedrich-Schiller-Universität Jena, Max-Wien-Platz 1, 07743 Jena, Germany

(Received 21 September 2004; published 31 January 2005)

We derive Keplerian-type parametrization for the solution of post-Newtonian (PN) accurate conservative dynamics of spinning compact binaries moving in eccentric orbits. The PN accurate dynamics that we consider consists of the third post-Newtonian accurate conservative orbital dynamics influenced by the leading order spin effects, namely, the leading order spin-orbit interactions. The orbital elements of the representation are explicitly given in terms of the conserved orbital energy, angular momentum, and a quantity that characterizes the leading order spin-orbit interactions in Arnowitt, Deser, and Misner-type coordinates. Our parametric solution is applicable in the following two distinct cases: (i) the binary consists of equal-mass compact objects, having two arbitrary spins, and (ii) the binary consists of compact objects of arbitrary mass, where only one of them is spinning with an arbitrary spin. As an application of our parametrization, we present gravitational-wave polarizations, whose amplitudes are restricted to the leading quadrupolar order, suitable to describe gravitational radiation from spinning compact binaries moving in eccentric orbits. The present parametrization will be required to construct ''ready to use'' reference templates for gravitational waves from spinning compact binaries in inspiralling eccentric orbits. Our parametric solution for the post-Newtonian accurate conservative dynamics of spinning compact binaries clearly indicates, for the cases considered, the absence of chaos in these systems. Finally, we note that our parametrization provides the first step in deriving a fully second post-Newtonian accurate ''timing formula'' that may be useful for the radio observations of relativistic binary pulsars such as J0737–3039.

DOI: 10.1103/PhysRevD.71.024039 PACS numbers: 04.25.Nx, 04.30.Db, 97.60.Jd, 97.60.Lf

I. INTRODUCTION

Inspiralling compact binaries of arbitrary mass ratio, consisting of black holes and neutron stars, are the most plausible sources of gravitational radiation for the commissioned ground-based and proposed space-based laser interferometric gravitational-wave detectors [1]. The possibility of detecting gravitational radiation from these sources is based on the following astrophysical and data analysis considerations. The detailed astrophysical investigations indicate that the inspiral of compact binaries should be observed by gravitational-wave detectors [2,3]. The temporally evolving gravitational-wave polarizations, $h_+(t)$ and $h_\times(t)$, associated with the inspiralling compact binaries in quasicircular orbits are known very precisely [4,5]. This allows data analysts to employ the optimal method of matched filtering to extract these weak gravitational-wave signals from the noisy interferometric data [6].

It should be noted that the construction of the ''ready to use search templates,'' namely, above mentioned $h_+(t)$ and $h_\times(t)$, is possible mainly due to the fact that the orbital dynamics, during the binary inspiral, is well described by the post-Newtonian (PN) approximation to general relativity. The PN approximation to general relativity allows one to express the equations of motion for a compact binary as corrections to Newtonian equations of motion in powers of $(v/c)^2 \sim GM/(c^2R)$, where v, M, and R are the characteristic orbital velocity, the total mass, and the typical orbital separation of the binary, respectively. At present, the orbital dynamics of nonspinning compact binaries is explicitly known to 3.5PN order, which gives $(v/c)^7$ corrections to Newtonian equations of motion. These lengthy high PN corrections were obtained, for the first time, in Arnowitt, Deser, and Misner (ADM)-type coordinates [7–10]. Independently, they were later computed in harmonic coordinates and, as expected, found to be in perfect agreement [11–16]. Further, we point out that the very recent determination of the highly desirable 3.5PN (relative) accurate phase evolution for the gravitational-wave polarizations was possible mainly because of employing techniques used in the computations of 3.5PN accurate equations of motion for the dynamics of compact binaries [9].

However, the effect of spins and orbital eccentricity on the compact binary dynamics and the associated $h_+(t)$ and $h_\times(t)$ is not so accurately determined. The dynamics of spinning compact binaries is determined not only by the orbital equations of motion for these objects, but also by the precession equations for the spin vectors themselves [17]. In fact, for the dynamics of spinning compact binaries only the leading order contributions to spin-orbit and spin-spin interactions are well understood [18,19]. It is therefore quite customary, in the existing literature, to consider only the leading order contributions to spin-orbit and spin-spin

*Electronic address: C.Koenigsdoerffer@uni-jena.de
†Electronic address: A.Gopakumar@uni-jena.de

interactions, while exploring the dynamics of spinning compact binaries [20] or the influence of spins on the phase evolution and amplitude modulations of the gravitational waveforms [21]. However, note that the equations of motion for spinning compact binaries, which include first post-Newtonian corrections to the leading order spin-orbit contributions, are also available [22]. The leading order spin effects on the gravitational-wave polarizations, mainly for compact binaries in quasicircular orbits, were also explored in great detail [23]. As far as the orbital eccentricity is considered, the temporally evolving $h_+(t)$ and $h_\times(t)$, whose amplitudes are Newtonian accurate and the orbital evolution is exactly 2.5PN accurate, were recently obtained [24]. However, the inputs required to compute the crucial secular phase evolution for compact binaries in inspiralling eccentric orbits are also available to 2PN order beyond the leading quadrupole contributions [24,25]. Further, very recently, a Keplerian-type parametrization for the solution of 3PN accurate equations of motion for two nonspinning compact objects moving in eccentric orbits was obtained [26]. It is therefore desirable to obtain a Keplerian-type parametric solution to the dynamics of compact binaries when spin effects are not neglected.

In this paper, we obtain a Keplerian-type parametric solution to the PN accurate dynamics of spinning compact binaries moving in eccentric orbits when the dynamics includes the leading spin-orbit interaction. Our parametric solution is applicable in the following two distinct cases: (i) the binary is composed of two compact objects of equal mass and two arbitrary spins, and (ii) the two objects have unequal masses but only one object has a spin. The present parametrization can easily be added to the recently obtained 3PN accurate generalized quasi-Keplerian parametrization for the solution of the 3PN accurate equations of motion for two nonspinning compact objects moving in eccentric orbits [26]. This will provide, for the first time, an almost analytic, 3PN accurate parametric solution to the dynamics of spinning compact binaries moving in eccentric orbits when the spin effects are restricted, for the time being, to the leading order spin-orbit contributions [27]. As an application of the parametrization, we present explicit expressions for the spin-orbit modulated $h_+(t)$ and $h_\times(t)$, whose amplitudes are restricted, for convenience, to the Newtonian order and the orbital motion is restricted to the above mentioned conservative PN order. Our results generalize and improve, for the two cases considered, a restricted parametrization for the orbital motion of compact binaries with leading order spin-orbit coupling [28].

Our parametrization will have the following possible applications. The construction of "ready to use" search templates, namely, $h_+(t)$ and $h_\times(t)$, for compact binaries in inspiralling orbits requires a detailed knowledge of the PN accurate orbital dynamics and a PN accurate description for $h_{ij}^{\rm TT}$, the transverse-traceless (TT) part of the radiation field. As mentioned earlier, time evolving $h_+(t)$ and $h_\times(t)$ for nonspinning compact binaries of arbitrary masses moving in inspiralling eccentric orbits were obtained in Ref. [24]. The parametrization presented here, along with Ref. [26], will be required to construct PN accurate ready to use reference templates for spinning compact binaries moving even in inspiralling eccentric orbits.

There is an ongoing debate about whether or not the spinning compact binaries, of arbitrary mass ratio, moving in circular or eccentric orbits under PN accurate dynamics will exhibit chaotic behavior [20]. The question of chaos was originally motivated by the observation that the equations describing the motion of a spinning test particle in Schwarzschild spacetime allow chaotic solutions [29]. The issue is usually addressed by solving numerically PN accurate equations describing the dynamics of spinning compact binaries to compute certain gauge dependent quantities such as fractal basin boundaries and Lyapunov exponents. The semianalytic parametrization presented here, along with the future extensions, should be very effective in analyzing the PN accurate dynamics of spinning compact binaries and exploring whether astrophysically realistic binary inspiral will be chaotic or not. Further, the parametrization for the cases considered implies that the associated PN accurate conservative binary dynamics cannot exhibit chaos.

Finally, we note that our parametrization may be useful to analyze the high precision radio-wave observations of relativistic binary pulsars such as J0737−3039 [30]. These radio-wave observations employ a "timing formula," which gives the arrival times at the barycenter of the solar system for the electromagnetic pulses emitted by a binary pulsar. The timing formula is important for obtaining astrophysical information from the compact binary as well as to test general relativity in strong field regimes [31,32]. The heavily employed timing formula usually incorporates 1PN accurate orbital motion, leading order secular effects due to gravitational radiation reaction, spin-orbit coupling as well as 2PN (secular) corrections to the advance of periastron [31,33–35]. The parametric solution obtained here will be required to obtain a 2PN accurate timing formula, where all spin-orbit and 2PN corrections are fully included. This implies a timing formula which includes not only 2PN order secular effects, but all 2PN order periodic terms, which may leave some potentially observable signature [28,36,37].

The paper is structured in the following manner. In Sec. II, we exhibit and explain, in detail, the total Hamiltonian describing the conservative dynamics, whose parametric solution we are seeking in this paper. In Sec. III, we summarize the Keplerian-type parametrization that describes the solution to the 3PN accurate equations of motion for compact binaries, in eccentric orbits when spin effects are ignored. Section IV describes the determination of a Keplerian-type parametrization for the conservative dynamics of spinning compact binaries when spin effects are restricted to the leading order spin-orbit interaction. The parametric solutions, presented in Secs. III and IV, are combined in Sec. V to obtain PN accurate Keplerian-type parametrization for the conservative dynamics of spinning compact binaries moving in eccentric orbits. As an application to our PN accurate parametric solution, we present explicit analytic expressions for the gravitational-wave polarizations, $h_+(t)$ and $h_\times(t)$, for spinning compact binaries in eccentric orbits in Sec. VI. The temporal evolution of $h_+(t)$ and $h_\times(t)$, whose amplitudes are Newtonian accurate, will be governed, for the time being, by the conservative PN dynamics discussed in this paper. Finally, in Sec. VII, we summarize our result and discuss its future extensions and applications.

II. DYNAMICS OF COMPACT BINARIES WITH LEADING ORDER SPIN-ORBIT INTERACTION

In this paper, as mentioned earlier, we are interested in the 3PN accurate conservative dynamics of spinning compact binaries when spin effects are, for the time being, restricted to the leading order spin-orbit interaction. The dynamics is fully specified by a post-Newtonian accurate Hamiltonian $\mathcal{H}$, which may be symbolically written as

$$\mathcal{H} = \mathcal{H}_{\rm N} + \mathcal{H}_{\rm 1PN} + \mathcal{H}_{\rm 2PN} + \mathcal{H}_{\rm 3PN} + \mathcal{H}_{\rm SO}, \quad (2.1)$$

where $\mathcal{H}_{\rm N}$, $\mathcal{H}_{\rm 1PN}$, $\mathcal{H}_{\rm 2PN}$, and $\mathcal{H}_{\rm 3PN}$ are, respectively, the Newtonian, first, second, and third post-Newtonian contributions to the conservative dynamics of compact binaries when the spin effects are neglected. The leading order spin-orbit coupling to the binary dynamics is given by $\mathcal{H}_{\rm SO}$. We determine the parametric solution to the dynamics, given by Eq. (2.1), in the following way. First, we obtain a parametric solution to the PN accurate conservative dynamics, neglecting the effects due to spin-orbit coupling. We then compute a parametric solution to the conservative dynamics, given by $\mathcal{H}_{\rm N} + \mathcal{H}_{\rm SO}$. The second step is consistent in a post-Newtonian framework as the spin-orbit interactions are restricted to the leading order. In the final step, we consistently combine these two parametrizations to obtain a PN accurate parametric solution to the conservative compact binary dynamics, as specified by $\mathcal{H}$.

In the present work, we employ the following 3PN accurate conservative Hamiltonian, in ADM-type coordinates [38,39], supplemented with a contribution describing the leading order spin-orbit coupling. We work, as is usual in the literature [26], with the following 3PN accurate conservative reduced Hamiltonian: $H = \mathcal{H}/\mu$, where the reduced mass of the binary is given by $\mu = m_1 m_2/M$, m_1 and m_2 being the individual masses and $M = m_1 + m_2$ is the total mass. The 3PN accurate (reduced) Hamiltonian, in ADM-type coordinates and in the center-of-mass frame, with the leading order spin-orbit contributions reads

$$H(\boldsymbol{r}, \boldsymbol{p}, \boldsymbol{S}_1, \boldsymbol{S}_2) = H_{\rm N}(\boldsymbol{r}, \boldsymbol{p}) + H_{\rm 1PN}(\boldsymbol{r}, \boldsymbol{p}) + H_{\rm 2PN}(\boldsymbol{r}, \boldsymbol{p}) + H_{\rm 3PN}(\boldsymbol{r}, \boldsymbol{p}) + H_{\rm SO}(\boldsymbol{r}, \boldsymbol{p}, \boldsymbol{S}_1, \boldsymbol{S}_2), \quad (2.2)$$

where the Newtonian, post-Newtonian, and spin-orbit contributions are given by

$$H_{\rm N}(\boldsymbol{r}, \boldsymbol{p}) = \frac{\boldsymbol{p}^2}{2} - \frac{1}{r}, \quad (2.3a)$$

$$H_{\rm 1PN}(\boldsymbol{r}, \boldsymbol{p}) = \frac{1}{c^2}\left\{\frac{1}{8}(3\eta - 1)(\boldsymbol{p}^2)^2 - \frac{1}{2}[(3+\eta)\boldsymbol{p}^2 + \eta(\boldsymbol{n}\cdot\boldsymbol{p})^2]\frac{1}{r} + \frac{1}{2r^2}\right\}, \quad (2.3b)$$

$$H_{\rm 2PN}(\boldsymbol{r}, \boldsymbol{p}) = \frac{1}{c^4}\left\{\frac{1}{16}(1 - 5\eta + 5\eta^2)(\boldsymbol{p}^2)^3 + \frac{1}{8}[(5 - 20\eta - 3\eta^2)(\boldsymbol{p}^2)^2 - 2\eta^2(\boldsymbol{n}\cdot\boldsymbol{p})^2\boldsymbol{p}^2 - 3\eta^2(\boldsymbol{n}\cdot\boldsymbol{p})^4]\frac{1}{r} + \frac{1}{2}[(5 + 8\eta)\boldsymbol{p}^2 + 3\eta(\boldsymbol{n}\cdot\boldsymbol{p})^2]\frac{1}{r^2} - \frac{1}{4}(1 + 3\eta)\frac{1}{r^3}\right\}, \quad (2.3c)$$

$$H_{\rm 3PN}(\boldsymbol{r}, \boldsymbol{p}) = \frac{1}{c^6}\bigg(\frac{1}{128}(-5 + 35\eta - 70\eta^2 + 35\eta^3)(\boldsymbol{p}^2)^4 + \frac{1}{16}[(-7 + 42\eta - 53\eta^2 - 5\eta^3)(\boldsymbol{p}^2)^3 + (2 - 3\eta)\eta^2(\boldsymbol{n}\cdot\boldsymbol{p})^2(\boldsymbol{p}^2)^2 + 3(1-\eta)\eta^2(\boldsymbol{n}\cdot\boldsymbol{p})^4\boldsymbol{p}^2 - 5\eta^3(\boldsymbol{n}\cdot\boldsymbol{p})^6]\frac{1}{r} + \left[\frac{1}{16}(-27 + 136\eta + 109\eta^2)(\boldsymbol{p}^2)^2 + \frac{1}{16}(17 + 30\eta)\eta(\boldsymbol{n}\cdot\boldsymbol{p})^2\boldsymbol{p}^2 + \frac{1}{12}(5 + 43\eta)\eta(\boldsymbol{n}\cdot\boldsymbol{p})^4\right]\frac{1}{r^2} + \left\{\frac{1}{192}[-600 + (3\pi^2 - 1340)\eta - 552\eta^2]\boldsymbol{p}^2 - \frac{1}{64}(340 + 3\pi^2 + 112\eta)\eta(\boldsymbol{n}\cdot\boldsymbol{p})^2\right\}\frac{1}{r^3} + \frac{1}{96}[12 + (872 - 63\pi^2)\eta]\frac{1}{r^4}\bigg), \quad (2.3d)$$

$$H_{\rm SO}(\boldsymbol{r}, \boldsymbol{p}, \boldsymbol{S}_1, \boldsymbol{S}_2) = \frac{1}{c^2 r^3}(\boldsymbol{r}\times\boldsymbol{p})\cdot\boldsymbol{S}_{\rm eff}. \quad (2.3e)$$

In the above equations $\boldsymbol{r} = \boldsymbol{\mathcal{R}}/(GM)$, $r = |\boldsymbol{r}|$, $\boldsymbol{n} = \boldsymbol{r}/r$, and $\boldsymbol{p} = \boldsymbol{\mathcal{P}}/\mu$, where $\boldsymbol{\mathcal{R}}$ and $\boldsymbol{\mathcal{P}}$ are the relative separation vector and its conjugate momentum vector, respectively. The finite mass ratio η is given by $\eta = \mu/M$. The spin-orbit coupling involves the effective spin $\boldsymbol{S}_{\mathrm{eff}}$, given by

$$\boldsymbol{S}_{\mathrm{eff}} = \delta_1 \boldsymbol{S}_1 + \delta_2 \boldsymbol{S}_2, \tag{2.4}$$

where

$$\delta_1 = 2\eta\left(1 + \frac{3m_2}{4m_1}\right) = \frac{\eta}{2} + \frac{3}{4}\left(1 - \sqrt{1 - 4\eta}\right), \tag{2.5a}$$

$$\delta_2 = 2\eta\left(1 + \frac{3m_1}{4m_2}\right) = \frac{\eta}{2} + \frac{3}{4}\left(1 + \sqrt{1 - 4\eta}\right). \tag{2.5b}$$

The reduced spin vectors $\boldsymbol{S}_1$ and $\boldsymbol{S}_2$ are related to the individual spins S_1 and S_2 by $\boldsymbol{S}_1 = S_1/(\mu GM)$ and $\boldsymbol{S}_2 = S_2/(\mu GM)$, respectively. We recall that $\boldsymbol{\mathcal{R}}$, $\boldsymbol{\mathcal{P}}$, S_1, and S_2 are canonical variables, such that the orbital variables commute with the spin variables, e.g., see Refs. [17,19].

The above definition of the effective spin $\boldsymbol{S}_{\mathrm{eff}}$ is identical to the quantity $\boldsymbol{\zeta}$, introduced in Ref. [28], and related to $\boldsymbol{S}_{\mathrm{eff}}|_{\mathrm{TD}}$, introduced in Ref. [19], by $2\boldsymbol{S}_{\mathrm{eff}}|_{\mathrm{TD}} = GM^2 \boldsymbol{S}_{\mathrm{eff}}$.

The PN corrections, associated with the motion of non-spinning compact binaries, are compiled using Refs. [9,40]. The spin-orbit contribution to H, available in Ref. [35], employs the spin-supplementary condition (SSC) of Pryce, Newton, and Wigner [41,42]. The SSC, which defines the central world line of each spinning body, adopted in this paper is given by

$$2S_{i0} + \frac{1}{c} S_{ij} U^j = 0 \qquad (i, j = 1, 2, 3), \tag{2.6}$$

where $S_{\mu\nu}$ is the spin tensor and U^μ the 4-velocity of the center of mass of the body. The spin 4-vector S_α is defined by

$$S_\alpha = -\frac{1}{2c} \varepsilon_{\alpha\beta\mu\nu} U^\beta S^{\mu\nu} \qquad (\alpha, \beta, \mu, \nu = 0, 1, 2, 3), \tag{2.7}$$

where $\varepsilon_{\alpha\beta\mu\nu}$ is the Levi-Civita tensor with $\varepsilon_{0123} = +1$. In the rest frame of the body ($U^\mu = c\delta_0^\mu$),

$$S_\alpha = (0, S^{23}, S^{31}, S^{12}) = (0, S) \tag{2.8}$$

holds. The spins, S_1 and S_2, of the compact objects may be given in terms of their moments of inertia and angular velocities of proper rotations, I_a and $\boldsymbol{\Omega}_a$ ($a = 1, 2$), respectively, as

$$S_1 = I_1 \boldsymbol{\Omega}_1, \tag{2.9a}$$

$$S_2 = I_2 \boldsymbol{\Omega}_2. \tag{2.9b}$$

Using the above definitions, it is possible to determine at what PN order the leading order spin-orbit interaction will manifest. It is easy to see, using Eq. (2.3), that spin effects enter the dynamics formally at 1PN order. However, for compact objects, the spin is roughly given by $S \sim m_{\mathrm{co}} r_{\mathrm{co}} v^{\mathrm{spin}} \sim G m_{\mathrm{co}}^2 v^{\mathrm{spin}}/c^2$, where m_{co}, r_{co}, and v^{spin} are the typical mass, size, and rotational velocity, respectively, of the spinning compact object. This implies, for moderate v^{spin} values, that the leading order spin-orbit coupling will enter the compact binary dynamics at $\mathcal{O}(1/c^4)$, i.e., at 2PN order. It is interesting to note that, if $v^{\mathrm{spin}} \sim c$, then the leading order spin-orbit interaction will numerically manifest at 1.5PN order. However, in that case the binary dynamics should be dominated by the currently neglected PN corrections to H_{SO}. In this paper, we will, for the sake of clarity and simplicity, assume that the spin-orbit interaction influences the compact binary dynamics at 2PN order. We point out that the present derivation of the Keplerian-type parametrization for the PN accurate dynamics of spinning compact binaries does not really care if the spin-orbit coupling manifests at 1.5PN or 2PN order.

In the next section, we will display and explain the recently obtained Keplerian-type parametric solution to the 3PN accurate conservative orbital motion of two compact objects, of negligible proper rotations, moving in eccentric orbits [26].

III. KEPLERIAN-TYPE PARAMETRIZATION FOR THE ORBITAL MOTION OF COMPACT BINARIES WITH NEGLIGIBLE PROPER ROTATION

Using the fully determined 3PN accurate conservative Hamiltonian, in ADM-type coordinates and in the center-of-mass frame, available in Refs. [9,40], very recently a Keplerian-type parametrization for the orbital motion of compact binaries in eccentric orbits was derived [26]. The derivation of the above parametric solution, usually referred to as the 3PN accurate generalized quasi-Keplerian parametrization, crucially depends on the following important points. First, the 3PN accurate conservative Hamiltonian is invariant under time translation and spatial rotations, implying the existence of 3PN accurate (reduced) energy $E = H$ and (reduced) orbital angular momentum $\boldsymbol{L} = \boldsymbol{r} \times \boldsymbol{p}$ for the binary in the center-of-mass frame. In particular, the conservation of $\boldsymbol{L}$ indicates that the motion is restricted to a plane, namely, the orbital plane, and we may introduce polar coordinates such that $\boldsymbol{r} = r(\cos\varphi, \sin\varphi)$. Finally, the Hamiltonian equations of motion governing the relative motion of the compact binary, namely, the 3PN accurate expressions for $\dot{r} = dr/dt$ and $\dot{\varphi} = d\varphi/dt$—where t denotes the coordinate time scaled by GM—in terms of $E, L = |\boldsymbol{L}|$ and r, are polynomials of degree seven in $1/r$.

The third post-Newtonian accurate generalized quasi-Keplerian parametrization for compact binaries moving in eccentric orbits, in ADM-type coordinates and in the center-of-mass frame, is given by

$$r = a_r(1 - e_r \cos u), \tag{3.1a}$$

$$l \equiv n(t - t_0) = u - e_t \sin u + \left(\frac{g_{4t}}{c^4} + \frac{g_{6t}}{c^6}\right)(v - u) + \left(\frac{f_{4t}}{c^4} + \frac{f_{6t}}{c^6}\right)\sin v + \frac{i_{6t}}{c^6}\sin 2v + \frac{h_{6t}}{c^6}\sin 3v, \tag{3.1b}$$

$$\varphi - \varphi_0 = (1 + k)v + \left(\frac{f_{4\varphi}}{c^4} + \frac{f_{6\varphi}}{c^6}\right)\sin 2v + \left(\frac{g_{4\varphi}}{c^4} + \frac{g_{6\varphi}}{c^6}\right)\sin 3v + \frac{i_{6\varphi}}{c^6}\sin 4v + \frac{h_{6\varphi}}{c^6}\sin 5v, \tag{3.1c}$$

$$\text{where} \quad v = 2\arctan\left[\left(\frac{1 + e_\varphi}{1 - e_\varphi}\right)^{1/2}\tan\frac{u}{2}\right]. \tag{3.1d}$$

The PN accurate orbital elements a_r, e_r^2, n, e_t^2, k, and e_φ^2 and the PN orbital functions g_{4t}, g_{6t}, f_{4t}, f_{6t}, i_{6t}, h_{6t}, $f_{4\varphi}$, $f_{6\varphi}$, $g_{4\varphi}$, $g_{6\varphi}$, $i_{6\varphi}$, and $h_{6\varphi}$ expressible in terms of E, L, and η are obtainable from Ref. [26] and will be explicitly displayed in Sec. V after including the effects due to the leading order spin-orbit interactions.

Let us make a few comments about the parametrization. The radial motion is uniquely parametrized by Eq. (3.1a) in terms of some PN accurate semimajor axis a_r, radial eccentricity e_r, and the eccentric anomaly u. The angular motion, described by Eq. (3.1c), is specified by the true anomaly v, angular eccentricity e_φ, advance of the periastron k, and some 2PN and 3PN order orbital functions. The explicit time dependence is provided by the 3PN accurate "Kepler equation," namely, Eq. (3.1b), which connects the mean anomaly l, and hence the coordinate time, to eccentric and true anomalies u and v, respectively. The PN accurate Kepler equation also includes some PN accurate mean motion n, time eccentricity e_t, and some 2PN and 3PN order orbital functions. It should be noted that all these eccentricities, e_r, e_φ, and e_t, are connected to each other by PN accurate expressions in terms of E, L, and η, given by Eq. (21) in Ref. [26]. This implies that it is possible to specify, as in the Newtonian case, a PN accurate eccentric orbit in terms of, for example, a_r and e_r. Finally, we recall that the Keplerian-type parametrization for compact binaries in eccentric orbits at first post-Newtonian order was obtained in Ref. [43]. Its extension to 2PN order was derived in Refs. [35,44].

In the next section, we will improve the above parametrization by including the effects due to the leading order spin-orbit interactions.

IV. QUASI-KEPLERIAN PARAMETRIZATION OF THE CONSERVATIVE DYNAMICS OF A SPINNING COMPACT BINARY—NEWTONIAN MOTION AUGMENTED BY THE FIRST-ORDER SPIN-ORBIT INTERACTION

In this section, we incorporate into the parametrization obtained in the previous section the effects due to the leading order spin-orbit coupling. The straightforward way of implementing that is to analyze the orbital dynamics, which is simply the Newtonian one augmented by the leading order spin-orbit interaction. Let us first describe, in the Hamiltonian framework, the binary dynamics in which we are interested.

A. The Newtonian binary dynamics with leading order spin effects

We investigate the binary dynamics, given by the reduced Hamiltonian $H_{\rm NSO}$, where $H_{\rm NSO} = H_{\rm N} + H_{\rm SO}$:

$$H_{\rm NSO} = \frac{\boldsymbol{p}^2}{2} - \frac{1}{r} + \frac{1}{c^2 r^3}\boldsymbol{L}\cdot\boldsymbol{S}_{\rm eff}. \tag{4.1}$$

The above Hamiltonian prescribes, via the Poisson brackets, the following evolution equations for the reduced angular momentum vector $\boldsymbol{L} = \boldsymbol{r}\times\boldsymbol{p}$ and the individual reduced spin vectors $\boldsymbol{S}_1$ and $\boldsymbol{S}_2$:

$$\frac{d\boldsymbol{L}}{dt} = \{\boldsymbol{L}, H_{\rm NSO}\} = \frac{1}{c^2 r^3}\boldsymbol{S}_{\rm eff}\times\boldsymbol{L}, \tag{4.2a}$$

$$\frac{d\boldsymbol{S}_1}{dt} = \{\boldsymbol{S}_1, H_{\rm NSO}\} = \frac{\delta_1}{c^2 r^3}\boldsymbol{L}\times\boldsymbol{S}_1, \tag{4.2b}$$

$$\frac{d\boldsymbol{S}_2}{dt} = \{\boldsymbol{S}_2, H_{\rm NSO}\} = \frac{\delta_2}{c^2 r^3}\boldsymbol{L}\times\boldsymbol{S}_2, \tag{4.2c}$$

where $\{\ldots,\ldots\}$ denotes the Poisson brackets. Note that $d\boldsymbol{L}/dt$, given by Eq. (4.2a), gives only the precessional motion of the orbital plane. We still need to obtain the equations describing the orbital motion. Before we go on to derive those equations, let us consider the conserved quantities associated with $H_{\rm NSO}$.

The reduced energy $E = H_{\rm NSO}$ is conserved because $\partial_t H_{\rm NSO} = 0$. Though $\boldsymbol{L}$ is not conserved, it is fairly easy to show that its magnitude $L = |\boldsymbol{L}|$ is conserved:

$$\frac{dL^2}{dt} = \frac{d}{dt}(\boldsymbol{L}\cdot\boldsymbol{L}) = \frac{2}{c^2 r^3}\boldsymbol{L}\cdot(\boldsymbol{S}_{\rm eff}\times\boldsymbol{L}) = 0. \tag{4.3}$$

Similarly, below we show that the magnitudes of the spins are also conserved:

$$\frac{dS_1^2}{dt} = \frac{d}{dt}(\boldsymbol{S}_1\cdot\boldsymbol{S}_1) = \frac{2\delta_1}{c^2 r^3}\boldsymbol{S}_1\cdot(\boldsymbol{L}\times\boldsymbol{S}_1) = 0, \tag{4.4a}$$

$$\frac{dS_2^2}{dt} = \frac{d}{dt}(\boldsymbol{S}_2\cdot\boldsymbol{S}_2) = \frac{2\delta_2}{c^2 r^3}\boldsymbol{S}_2\cdot(\boldsymbol{L}\times\boldsymbol{S}_2) = 0. \tag{4.4b}$$

Note that Eqs. (4.2) indicate that $\dot{\boldsymbol{S}} = -\dot{\boldsymbol{L}}$, where $\boldsymbol{S} = \boldsymbol{S}_1 + \boldsymbol{S}_2$ is the total spin reduced by μGM, the reduced total spin. We now define the conserved (reduced) total angular momentum vector

$$\boldsymbol{J} = \boldsymbol{L} + \boldsymbol{S}. \tag{4.5}$$

The above expression times μGM gives the total angular momentum $\boldsymbol{J}$, namely, $\boldsymbol{J} = \boldsymbol{\mathcal{R}} \times \boldsymbol{\mathcal{P}} + \boldsymbol{S}$. Moreover, $\boldsymbol{J}$ is conserved in both its magnitude and direction as $d\boldsymbol{J}/dt = 0$ and $dJ/dt = 0$, where $J = |\boldsymbol{J}|$.

The fact that $d\boldsymbol{J}/dt = 0$ allows us to introduce a reference orthonormal triad $(\boldsymbol{e}_X, \boldsymbol{e}_Y, \boldsymbol{e}_Z)$, such that $\boldsymbol{e}_Z$ is along the fixed vector $\boldsymbol{J}$. This gives

$$\boldsymbol{J} = J\boldsymbol{e}_Z. \tag{4.6}$$

Further, for later use, we choose the line-of-sight unit vector $\boldsymbol{N}$ to lie in the $\boldsymbol{e}_Y$-$\boldsymbol{e}_Z$ plane (see Fig. 1). This is always possible and reasonable because of the degree of freedom associated with the choice of $\boldsymbol{e}_X$ and $\boldsymbol{e}_Y$. These unit vectors $\boldsymbol{e}_X$ and $\boldsymbol{e}_Y$ span the invariable plane which is the plane perpendicular to $\boldsymbol{J}$.

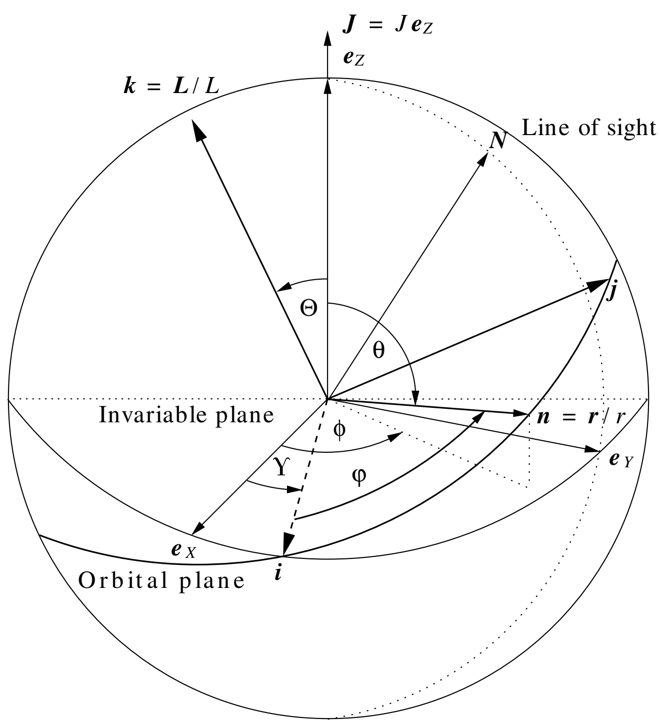

FIG. 1. The binary geometry and interpretations of various angles appearing in this section. Our reference frame is $(\boldsymbol{e}_X, \boldsymbol{e}_Y, \boldsymbol{e}_Z)$, where the basic vector $\boldsymbol{e}_Z$ is aligned with the fixed total angular momentum vector $\boldsymbol{J} = \boldsymbol{L} + \boldsymbol{S}$, such that $\boldsymbol{J} = J\boldsymbol{e}_Z$. The invariable plane $(\boldsymbol{e}_X, \boldsymbol{e}_Y)$ is perpendicular to $\boldsymbol{J}$. Important for the observation is the line-of-sight unit vector $\boldsymbol{N}$ from the observer to the source (compact binary). We may have, by a clever choice of $\boldsymbol{e}_X$ and $\boldsymbol{e}_Y$, the line-of-sight unit vector $\boldsymbol{N}$ in the $\boldsymbol{e}_Y$-$\boldsymbol{e}_Z$ plane. $\boldsymbol{k} = \boldsymbol{L}/L$ is the unit vector in the direction of the orbital angular momentum $\boldsymbol{L}$, which is perpendicular to the orbital plane. The constant inclination of the orbital plane with respect to the invariable plane is Θ, which is also the precession cone angle of $\boldsymbol{L}$ around $\boldsymbol{J}$. The orbital plane intersects the invariable plane at the line of nodes $\boldsymbol{i}$, with the longitude Υ measured in the invariable plane from $\boldsymbol{e}_X$. Υ is also the phase of the orbital plane precession. The orbital plane is spanned by the basic vectors $(\boldsymbol{i}, \boldsymbol{j})$, where $\boldsymbol{j} = \boldsymbol{k} \times \boldsymbol{i}$.

We now introduce highly advantageous spherical (polar) coordinates (r, θ, ϕ) and the associated orthonormal triad $(\boldsymbol{n}, \boldsymbol{e}_\theta, \boldsymbol{e}_\phi)$, where θ is the angle between $\boldsymbol{e}_Z$ and $\boldsymbol{n}$, and ϕ is the azimuthal angle defined in the invariable $\boldsymbol{e}_X$-$\boldsymbol{e}_Y$ plane (see Fig. 1), such that

$$\boldsymbol{n} = \sin\theta\cos\phi\boldsymbol{e}_X + \sin\theta\sin\phi\boldsymbol{e}_Y + \cos\theta\boldsymbol{e}_Z. \tag{4.7}$$

The relative separation vector $\boldsymbol{r}$ and its time derivative $\dot{\boldsymbol{r}} = d\boldsymbol{r}/dr$ written in the orthonormal triad $(\boldsymbol{n}, \boldsymbol{e}_\theta, \boldsymbol{e}_\phi)$ reads

$$\boldsymbol{r} = r\boldsymbol{n}, \tag{4.8a}$$

$$\dot{\boldsymbol{r}} = \dot{r}\boldsymbol{n} + r\dot{\theta}\boldsymbol{e}_\theta + r\sin\theta\dot{\phi}\boldsymbol{e}_\phi, \tag{4.8b}$$

In spherical coordinates, the linear momentum $\boldsymbol{p}$ and its magnitude may be expressed as

$$\boldsymbol{p} = p_r\boldsymbol{n} + p_\theta\boldsymbol{e}_\theta + p_\phi\boldsymbol{e}_\phi, \tag{4.9a}$$

$$\begin{aligned}\boldsymbol{p}^2 &= p_r^2 + p_\theta^2 + p_\phi^2 = (\boldsymbol{n}\cdot\boldsymbol{p})^2 + (\boldsymbol{n}\times\boldsymbol{p})^2\\ &= p_r^2 + \frac{L^2}{r^2}.\end{aligned} \tag{4.9b}$$

With the help of these relations and $E = H_{\rm NSO}$, the components of the linear momentum $\boldsymbol{p}$ can be expressed using the quantities E, L, and $(\boldsymbol{L}\cdot\boldsymbol{S}_{\rm eff})$ as

$$p_r^2 = 2E + \frac{2}{r} - \frac{L^2}{r^2} - \frac{2(\boldsymbol{L}\cdot\boldsymbol{S}_{\rm eff})}{c^2r^3}, \tag{4.10a}$$

$$p_\phi = \frac{L_Z}{r\sin\theta}, \tag{4.10b}$$

$$p_\theta^2 = \frac{L^2}{r^2} - p_\phi^2 = \frac{1}{r^2}\left(L^2 - \frac{L_Z^2}{\sin^2\theta}\right), \tag{4.10c}$$

where $L_Z = \boldsymbol{e}_Z\cdot\boldsymbol{L}$. Note that, in general, L_Z is not conserved.

The components of $\dot{\boldsymbol{r}}$ in the spherical polar coordinates, which also define the orbital equations of motion associated with $H_{\rm NSO}$, read

$$\dot{r} = \boldsymbol{n}\cdot\dot{\boldsymbol{r}} = p_r, \tag{4.11a}$$

$$r\dot{\theta} = \boldsymbol{e}_\theta\cdot\dot{\boldsymbol{r}} = p_\theta + \frac{\boldsymbol{e}_\phi\cdot\boldsymbol{S}_{\rm eff}}{c^2r^2}, \tag{4.11b}$$

$$r\sin\theta\dot{\phi} = \boldsymbol{e}_\phi\cdot\dot{\boldsymbol{r}} = p_\phi - \frac{\boldsymbol{e}_\theta\cdot\boldsymbol{S}_{\rm eff}}{c^2r^2}. \tag{4.11c}$$

In the above equations, we have used Hamilton's equation $\dot{\boldsymbol{r}} = \partial H_{\rm NSO}/\partial\boldsymbol{p}$, $\boldsymbol{n}\times\boldsymbol{e}_\theta = \boldsymbol{e}_\phi$, and $\boldsymbol{n}\times\boldsymbol{e}_\phi = -\boldsymbol{e}_\theta$.

Summarizing, we note that the dynamics of the binary system, described by the Hamiltonian $H_{\rm NSO}$, is also uniquely determined by the evolution equations given by Eqs. (4.2) and (4.11). Before trying to find parametric solutions to these equations, let us point out several features of the above binary dynamics.

It is easy to write down the precessional equations for the (reduced) total spin $\boldsymbol{S}$ and the effective spin $\boldsymbol{S}_{\rm eff}$ as

$$\dot{S} = \dot{S}_1 + \dot{S}_2 = \frac{1}{c^2 r^3} L \times S_{\rm eff} = -\dot{L}, \tag{4.12a}$$

$$\dot{S}_{\rm eff} = \delta_1 \dot{S}_1 + \delta_2 \dot{S}_2 = \frac{1}{c^2 r^3} L \times (\delta_1^2 S_1 + \delta_2^2 S_2). \tag{4.12b}$$

It is clear that the motions of S and $S_{\rm eff}$ are more complicated than those for S_1 and S_2. We deduce that the magnitudes of S and $S_{\rm eff}$ are not preserved in general and satisfy the following equations:

$$\frac{dS^2}{dt} = -\frac{3\sqrt{1-4\eta}}{c^2 r^3} L \cdot (S_1 \times S_2), \tag{4.13a}$$

$$\frac{dS_{\rm eff}^2}{dt} = -\frac{3\sqrt{1-4\eta}(12\eta + \eta^2)}{4c^2 r^3} L \cdot (S_1 \times S_2). \tag{4.13b}$$

We note that the quantity $(L \cdot S_{\rm eff})$ is exactly preserved since

$$\frac{d}{dt}(L \cdot S_{\rm eff}) = \frac{dL}{dt} \cdot S_{\rm eff} + L \cdot \frac{dS_{\rm eff}}{dt} = 0. \tag{4.14}$$

Finally, let us consider the evolution of L_Z. Using $L = J e_Z - S$ on the right-hand side of Eq. (4.2a), we obtain

$$\frac{dL_Z}{dt} = \frac{3\sqrt{1-4\eta}}{2c^2 r^3} e_Z \cdot (S_1 \times S_2). \tag{4.15}$$

The above equations imply that, in general, L_Z is not conserved. However, L_Z along with S and $S_{\rm eff}$ are conserved for the following two cases. In the first instance, case (i), we require the binary to have equal masses, but with arbitrary spins S_1 and S_2 ($m_1 = m_2 \Leftrightarrow \eta = 1/4 \Leftrightarrow \delta_1 = \delta_2$). In the second instance, case (ii), the binary may have arbitrary masses, but only *one* of them is spinning ($m_1 \neq m_2$, $S_1 \neq 0$ *or* $S_2 \neq 0$).

In this paper, when we solve the differential equations, Eqs. (4.2) and (4.11), we restrict ourselves, for the time being, to the above two cases. In these cases, the effective spin $S_{\rm eff}$ and the reduced total spin S are related by

$$S_{\rm eff} = \delta_1 S_1 + \delta_2 S_2 = \chi_{\rm so} S, \tag{4.16}$$

where the newly defined mass dependent coupling constant $\chi_{\rm so}$ is given by

$$\chi_{\rm so} := \begin{cases} \delta_1 = \delta_2 = 7/8 & \text{for (i), the equal-mass case,} \\ \delta_1 \text{ or } \delta_2 & \text{for (ii), the single-spin case.} \end{cases}$$

We emphasize that in case (i) the reduced total spin S is the sum of two arbitrary spins S_1 and S_2. However, in case (ii) S is either S_1 *or* S_2.

These observations allow us to present the precessional equations for L and S in the following compact form for the special cases:

$$\frac{dL}{dt} = \frac{\chi_{\rm so}}{c^2 r^3} J \times L, \tag{4.17a}$$

$$\frac{dS}{dt} = \frac{\chi_{\rm so}}{c^2 r^3} J \times S. \tag{4.17b}$$

Equations (4.17) imply that the (reduced) orbital angular momentum L and the (reduced) total spin S, for the two cases considered, precess about the fixed vector $J = J e_Z$ at the same rate with an (instantaneous) precession frequency given by

$$\omega_p = \frac{\chi_{\rm so} J}{c^2 r^3}. \tag{4.18}$$

Note that ω_p can only be defined in a *physically* meaningful way when spin effects are included in the binary dynamics. In the nonspinning limit, the cross products appearing on the right-hand side of Eqs. (4.17) vanish, leaving the (reduced) orbital angular momentum L as a constant vector. It is interesting to observe that, in the nonspinning limit, neither ω_p nor $\chi_{\rm so}$ go to zero.

In the next subsection, we will find a parametric solution to the dynamics of spinning compact binaries in eccentric orbits, given by Eqs. (4.11) and (4.17).

B. The Keplerian-type parametrization associated with the Hamiltonian $H_{\rm NSO}$

We start by considering the radial motion, governed by Eq. (4.11a), which reads

$$\dot{r}^2 = 2E + \frac{2}{r} - \frac{L^2}{r^2} - \frac{2(L \cdot S_{\rm eff})}{c^2 r^3}. \tag{4.19}$$

We obtain the parametric solution to the above equation by following exactly the same procedure described in detail in Sec. III of Ref. [26]. The radial motion is described by

$$r = a_r(1 - e_r \cos u), \tag{4.20a}$$

$$l \equiv n(t - t_0) = u - e_t \sin u, \tag{4.20b}$$

where u and l are the eccentric and mean anomalies, respectively. The orbital elements, explicitly given in terms of E, L, and $L \cdot S_{\rm eff}$, are

$$a_r = -\frac{1}{2E}\left(1 - 2\frac{L \cdot S_{\rm eff}}{L^2}\frac{E}{c^2}\right), \tag{4.21a}$$

$$e_r^2 = 1 + 2EL^2 + 8(1 + EL^2)\frac{L \cdot S_{\rm eff}}{L^2}\frac{E}{c^2}, \tag{4.21b}$$

$$n = (-2E)^{3/2}, \tag{4.21c}$$

$$e_t^2 = 1 + 2EL^2 + 4\frac{L \cdot S_{\rm eff}}{L^2}\frac{E}{c^2}. \tag{4.21d}$$

Equation (4.20b) gives the Kepler equation, modified by the spin-orbit interaction, which connects the eccentric anomaly u to the coordinate time. The crucial requirements to determine the above parametrization are the conservation of E, L, and $L \cdot S_{\rm eff}$. This allows us to treat $(dr/dt)^2$ as a polynomial in $1/r$ with constant coefficients.

Let us now find the parametric solution to the angular parts of the orbital equations of motion, Eqs. (4.11) combined with Eq. (4.16), written in the form

$$r\dot{\theta} = p_\theta\left(1 - \frac{\chi_{so}}{c^2 r}\right), \tag{4.22a}$$

$$r\sin\theta\dot{\phi} = p_\phi\left(1 - \frac{\chi_{so}}{c^2 r}\right) + \frac{\chi_{so} J \sin\theta}{c^2 r^2}. \tag{4.22b}$$

For the cases of interest, where L_Z is a constant, we may introduce a constant angle Θ between $\boldsymbol{e}_Z$ and $\boldsymbol{L}$ such that $L_Z = L\cos\Theta$ (see Fig. 1) and Eqs. (4.10b) and (4.10c) simplify to

$$p_\phi = \frac{L}{r}\frac{\cos\Theta}{\sin\theta}, \tag{4.23a}$$

$$p_\theta^2 = \frac{L^2}{r^2}\left(1 - \frac{\cos^2\Theta}{\sin^2\theta}\right). \tag{4.23b}$$

The efficient way of determining the solution to Eqs. (4.22) begins by expressing the radial vector $\boldsymbol{r}$ in terms of an orbital triad. This is achieved by connecting via two rotations the reference triad $(\boldsymbol{e}_X, \boldsymbol{e}_Y, \boldsymbol{e}_Z)$ to an orbital triad defined by $(\boldsymbol{i}, \boldsymbol{j}, \boldsymbol{k})$. In our orbital orthonormal triad, the unit vector $\boldsymbol{k}$, given by $\boldsymbol{k} = \boldsymbol{L}/L$, along with $\boldsymbol{e}_Z$ defines

$$\boldsymbol{i} = \frac{\boldsymbol{e}_Z \times \boldsymbol{k}}{|\boldsymbol{e}_Z \times \boldsymbol{k}|}. \tag{4.24}$$

Note that $|\boldsymbol{e}_Z \times \boldsymbol{k}| = \sin\Theta$, which is indeed always positive because $0 \leq \Theta < \pi$. We note that the unit vector $\boldsymbol{i}$ gives the line of nodes associated with the intersection of the orbital plane with the invariable plane $(\boldsymbol{e}_X, \boldsymbol{e}_Y)$. The corresponding inclination angle is Θ. Since the above mentioned line of nodes vanishes in the nonspinning limit, the unit vector $\boldsymbol{i}$ is defined only when spin effects are included in the binary dynamics.

The two rotations arise from the observation that the (instantaneous) position and orientation of the orbital plane with respect to the reference triad $(\boldsymbol{e}_X, \boldsymbol{e}_Y, \boldsymbol{e}_Z)$ are defined by two angles: the longitude of the line of nodes Υ ($0 \leq \Upsilon < 2\pi$) and the inclination of the orbital plane with respect to the invariable $\boldsymbol{e}_X$-$\boldsymbol{e}_Y$ plane Θ ($0 \leq \Theta < \pi$). In terms of rotational matrices, we have

$$\begin{pmatrix} \boldsymbol{i} \\ \boldsymbol{j} \\ \boldsymbol{k} \end{pmatrix} = \begin{pmatrix} 1 & 0 & 0 \\ 0 & \cos\Theta & \sin\Theta \\ 0 & -\sin\Theta & \cos\Theta \end{pmatrix} \begin{pmatrix} \cos\Upsilon & \sin\Upsilon & 0 \\ -\sin\Upsilon & \cos\Upsilon & 0 \\ 0 & 0 & 1 \end{pmatrix} \times \begin{pmatrix} \boldsymbol{e}_X \\ \boldsymbol{e}_Y \\ \boldsymbol{e}_Z \end{pmatrix}.$$

In the new orbital orthonormal triad $(\boldsymbol{i}, \boldsymbol{j}, \boldsymbol{k})$, the relative separation vector $\boldsymbol{r}$ is given by

$$\boldsymbol{r} = r\cos\varphi \boldsymbol{i} + r\sin\varphi \boldsymbol{j}, \tag{4.25}$$

where the unit vectors $(\boldsymbol{i}, \boldsymbol{j}, \boldsymbol{k})$ in terms of the reference triad $(\boldsymbol{e}_X, \boldsymbol{e}_Y, \boldsymbol{e}_Z)$ are explicitly given by

$$\boldsymbol{i} = \cos\Upsilon \boldsymbol{e}_X + \sin\Upsilon \boldsymbol{e}_Y, \tag{4.26a}$$

$$\boldsymbol{j} = -\cos\Theta\sin\Upsilon \boldsymbol{e}_X + \cos\Theta\cos\Upsilon \boldsymbol{e}_Y + \sin\Theta \boldsymbol{e}_Z, \tag{4.26b}$$

$$\boldsymbol{k} = \sin\Theta\sin\Upsilon \boldsymbol{e}_X - \sin\Theta\cos\Upsilon \boldsymbol{e}_Y + \cos\Theta \boldsymbol{e}_Z, \tag{4.26c}$$

The geometrical interpretations of the newly introduced angles and basic vectors are illustrated in Fig. 1.

The comparison of $\boldsymbol{r}$, given by Eqs. (4.8a) and (4.7), with the one in the new angular variables, Eq. (4.25) with Eqs. (4.26), implies the following transformations for the angular variables:

$$(\theta, \phi) \rightarrow (\Upsilon, \varphi): \begin{cases} \cos\theta = \sin\varphi\sin\Theta \\ \sin(\phi - \Upsilon)\sin\theta = \sin\varphi\cos\Theta \\ \cos(\phi - \Upsilon)\sin\theta = \cos\varphi \end{cases}. \tag{4.27}$$

A clever combination of the above angular transformation equations and their corresponding time derivatives leads to the following relations for the angular velocities:

$$\dot{\theta}^2 = \left(1 - \frac{\cos^2\Theta}{\sin^2\theta}\right)\dot{\varphi}^2, \tag{4.28a}$$

$$\dot{\phi} = \dot{\Upsilon} + \frac{\cos\Theta}{\sin^2\theta}\dot{\varphi}, \tag{4.28b}$$

where the over dot again means the derivative with respect to time t and Θ is treated as a constant angle.

Using Eq. (4.28a) for $\dot{\theta}^2$ in Eq. (4.22a) with (4.23b) leads to

$$\dot{\varphi} = \frac{L}{r^2}\left(1 - \frac{\chi_{so}}{c^2 r}\right). \tag{4.29}$$

Note that the above derivation requires $\Theta \neq 0$, which is always satisfied for $\boldsymbol{S} \neq 0$, and hence Eq. (4.29) is not defined when $\Theta = 0$. We again invoke the procedure employed in Sec. III of Ref. [26] to obtain the following parametric solution for φ:

$$\varphi - \varphi_0 = (1 + k)v, \tag{4.30a}$$

$$v = 2\arctan\left[\left(\frac{1 + e_\varphi}{1 - e_\varphi}\right)^{1/2}\tan\frac{u}{2}\right], \tag{4.30b}$$

where φ_0 is the value of φ at time t_0. The quantity k is a measure of the advance of the periastron and e_φ is the so-called angular eccentricity. They are expressible in terms of E, L, and $\boldsymbol{L} \cdot \boldsymbol{S}_{\mathrm{eff}}$ as

$$k = \frac{1}{c^2 L^2}\left(\chi_{so} - 3\frac{\boldsymbol{L} \cdot \boldsymbol{S}_{\mathrm{eff}}}{L^2}\right), \tag{4.31a}$$

$$e_\varphi^2 = 1 + 2EL^2 - 4\chi_{so}(1 + 2EL^2)\frac{E}{c^2} + 4(3 + 4EL^2)\frac{\boldsymbol{L} \cdot \boldsymbol{S}_{\mathrm{eff}}}{L^2}\frac{E}{c^2}. \tag{4.31b}$$

The parametrization for r, l, and φ can also be obtained using the *conchoidal* transformations employed in Ref. [33] and found to be in total agreement.

We now move on to derive the time evolution of Υ, the longitude of the line of intersection (denoted by the line of nodes unit vector $\boldsymbol{i}$ in Fig. 1) in a parametric way. Using Eq. (4.28b) for $\dot{\phi}$ with Eq. (4.29) in Eq. (4.22b) with Eq. (4.23a), we get the following differential equation for Υ:

$$\frac{d\Upsilon}{dt} = \frac{\chi_{\rm so} J}{c^2 r^3}, \qquad (4.32)$$

which is also restricted to the spinning case ($\Theta \neq 0$), since we made use of Eq. (4.29) for $\dot{\varphi}$.

Note that the right-hand side of the above equation is identical to ω_p, given by Eq. (4.18). This is not surprising as the frequencies of the precessional motion for $\boldsymbol{k} = \boldsymbol{L}/L$ and $\boldsymbol{i}$ should be identical due to Eqs. (4.24) and (4.26). Further, a close inspection of Fig. 1 reveals that the phase of the projection of $\boldsymbol{k}$ onto the invariable plane $(\boldsymbol{e}_X, \boldsymbol{e}_Y)$, as measured from $\boldsymbol{e}_X$, is given by $\Upsilon + 270°$.

To solve the differential Eq. (4.32) analytically, we divide it by $d\varphi/dt$, given by Eq. (4.29), and deduce at the leading order

$$\frac{d\Upsilon}{d\varphi} = \frac{\chi_{\rm so} J}{L} \frac{1}{c^2 r}. \qquad (4.33)$$

The radial separation r appearing on the right-hand side of the above equation may be replaced by the following expression in terms of v as shown below:

$$r = a(1 - e\cos u) = \frac{a(1-e^2)}{1 + e\cos v} = \frac{L^2}{1 + e\cos v}, \qquad (4.34)$$

where a and e may be treated as the Newtonian accurate expressions for a_r and e_r, respectively.

This allows us to write Eq. (4.33)—within the accuracy needed—as

$$\frac{d\Upsilon}{dv} = \frac{\chi_{\rm so} J}{c^2 L^3}(1 + e\cos v), \qquad (4.35)$$

where we also used the fact that $\varphi = v$ at the leading order. Equation (4.35) is easily integrated to obtain the parametric solution to Υ as

$$\Upsilon - \Upsilon_0 = \frac{\chi_{\rm so} J}{c^2 L^3}(v + e\sin v), \qquad (4.36)$$

where we put $v(t_0) = 0$.

There exists an alternate way to obtain $d\Upsilon/dt$, given by Eq. (4.32). Noting that the time evolution for the unit vector $\boldsymbol{k}$, defined by Eq. (4.26c), is solely given by that for Υ, we compute the time derivative of $\boldsymbol{k}$ and it reads

$$\dot{\boldsymbol{k}} = \dot{\Upsilon}\sin\Theta(\cos\Upsilon \boldsymbol{e}_X + \sin\Upsilon \boldsymbol{e}_Y). \qquad (4.37)$$

Using the fact that $\boldsymbol{L} = L\boldsymbol{k}$ and $\dot{\boldsymbol{L}} = L\dot{\boldsymbol{k}}$ in Eq. (4.17a), we arrive (again) at $d\Upsilon/dt$, as given by Eq. (4.32). Therefore, the parametric solution for Υ readily defines a similar solution for $\boldsymbol{L} = L\boldsymbol{k}$, where $\boldsymbol{k}$ is given by Eq. (4.26c) with (4.36). The parametric solution to $\boldsymbol{L}$ reads

$$\boldsymbol{L} = L(\sin\Theta\sin\Upsilon \boldsymbol{e}_X - \sin\Theta\cos\Upsilon \boldsymbol{e}_Y + \cos\Theta \boldsymbol{e}_Z). \qquad (4.38)$$

Finally, let us derive a parametric solution to the precessional motion of $\boldsymbol{S}$, given by Eq. (4.17b). This parametric solution follows immediately by noting that $\boldsymbol{S} = \boldsymbol{J} - \boldsymbol{L}$, where $\boldsymbol{J} = J\boldsymbol{e}_Z$ and $\boldsymbol{L} = L\boldsymbol{k}$. Using Eq. (4.26c) for $\boldsymbol{k}$, we deduce that

$$\boldsymbol{S} = L\sin\Theta(-\sin\Upsilon)\boldsymbol{e}_X + L\sin\Theta\cos\Upsilon \boldsymbol{e}_Y + (J - L\cos\Theta)\boldsymbol{e}_Z. \qquad (4.39)$$

The above equation, along with the parametric solution for Υ, describes, in a parametric way, the time evolution of $\boldsymbol{S}$.

We finally collect all the relevant equations, namely, Eqs. (4.20), (4.30), and (4.36), and display below our *parametric solution for the binary dynamics* given by $H_{\rm NSO}$:

$$\boldsymbol{r} = r\cos\varphi \boldsymbol{i} + r\sin\varphi \boldsymbol{j}, \qquad (4.40)$$

$$\boldsymbol{L} = L\boldsymbol{k}, \qquad (4.41)$$

$$\boldsymbol{S} = J\boldsymbol{e}_Z - L\boldsymbol{k}, \qquad (4.42)$$

where the basic vectors $(\boldsymbol{i}, \boldsymbol{j}, \boldsymbol{k})$ are explicitly given by

$$\boldsymbol{i} = \cos\Upsilon \boldsymbol{e}_X + \sin\Upsilon \boldsymbol{e}_Y, \qquad (4.43a)$$

$$\boldsymbol{j} = -\cos\Theta\sin\Upsilon \boldsymbol{e}_X + \cos\Theta\cos\Upsilon \boldsymbol{e}_Y + \sin\Theta \boldsymbol{e}_Z, \qquad (4.43b)$$

$$\boldsymbol{k} = \sin\Theta\sin\Upsilon \boldsymbol{e}_X - \sin\Theta\cos\Upsilon \boldsymbol{e}_Y + \cos\Theta \boldsymbol{e}_Z. \qquad (4.43c)$$

The time evolution for the radial and angular variables is given by

$$r = a_r(1 - e_r\cos u), \qquad (4.55a)$$

$$n(t - t_0) = u - e_t\sin u, \qquad (4.44b)$$

$$\varphi - \varphi_0 = (1 + k)v, \qquad (4.44c)$$

$$\Upsilon - \Upsilon_0 = \frac{\chi_{\rm so} J}{c^2 L^3}(v + e\sin v), \qquad (4.44d)$$

$$v = 2\arctan\left[\left(\frac{1 + e_\varphi}{1 - e_\varphi}\right)^{1/2}\tan\frac{u}{2}\right], \qquad (4.44e)$$

where the orbital elements are given by

$$a_r = -\frac{1}{2E}\left(1 - 2\chi_{\rm so}\cos\alpha\frac{S}{L}\frac{E}{c^2}\right), \tag{4.45a}$$

$$e_r^2 = 1 + 2EL^2 + 8(1 + EL^2)\chi_{\rm so}\cos\alpha\frac{S}{L}\frac{E}{c^2}, \tag{4.45b}$$

$$n = (-2E)^{3/2}, \tag{4.45c}$$

$$e_t^2 = 1 + 2EL^2 + 4\chi_{\rm so}\cos\alpha\frac{S}{L}\frac{E}{c^2}, \tag{4.45d}$$

$$k = \frac{1}{c^2L^2}\left(\chi_{\rm so} - 3\chi_{\rm so}\cos\alpha\frac{S}{L}\right), \tag{4.45e}$$

$$e_\varphi^2 = 1 + 2EL^2 - 4(1 + 2EL^2)\chi_{\rm so}\frac{E}{c^2} + 4(3 + 4EL^2)\chi_{\rm so}\cos\alpha\frac{S}{L}\frac{E}{c^2}. \tag{4.45f}$$

As noted earlier, e is given by the Newtonian contribution to e_r. In Eqs. (4.45), we have replaced $\boldsymbol{L}\cdot\boldsymbol{S}_{\rm eff}$ by $\chi_{\rm so}LS\cos\alpha$, where α is the constant angle between $\boldsymbol{L}$ and $\boldsymbol{S}$ and $\chi_{\rm so}$ is given by

$$\chi_{\rm so} := \begin{cases} \delta_1 = \delta_2 = 7/8 & \text{for (i), the equal-mass case,} \\ \delta_1 \text{ or } \delta_2 & \text{for (ii), the single-spin case.} \end{cases}$$

Further, we note that the constant angle Θ is not a free variable and is given by one of the following relations:

$$\sin\Theta = \frac{S\sin\alpha}{J}, \tag{4.46a}$$

$$\cos\Theta = \frac{L + S\cos\alpha}{J}, \tag{4.46b}$$

where the magnitude of the (reduced) total angular momentum is given by $J = (L^2 + S^2 + 2LS\cos\alpha)^{1/2}$.

We are aware that the above parametrization does not lead to the classic Keplerian parametrization simply by putting $S = 0$. There are several arguments for this apparent lack of a simple nonspinning limit. Notice that Υ and φ are defined with respect to the line of intersection, characterized by the line of nodes unit vector $\boldsymbol{i}$. When the spin effects are neglected, the above line of intersection disappears, since the orbital plane becomes the invariable plane and the associated inclination angle Θ vanishes. In this case, the related angles Υ and φ are not individually defined, though Eq. (4.27) gives us $\varphi + \Upsilon = \phi$, as required. We emphasize that the related differential equations, given by Eqs. (4.29) and (4.32), are obtained using $\Theta \neq 0$, corresponding to $S \neq 0$. Therefore, Eqs. (4.29) and (4.32) are not defined if $\Theta = 0$. Further, the apparent nonvanishing of the time evolution of Υ in the nonspinning limit is also attributable to the similar behavior for ω_p. However, a close scrutiny of Eqs. (4.19) and (4.22) with (4.23), (4.27), and (4.28) for $S \to 0$, which implies $\Theta \to 0$ and $\theta \to \pi/2$, reveals that the binary dynamics in the nonspinning case is describable in terms of r and ϕ, where $\phi = \varphi + \Upsilon$, as explained earlier.

Our parametric solution generalizes a restricted analysis considered in Ref. [28]. The analysis given in Ref. [28] neglects the precessional motion of the spin vectors and restricts $\boldsymbol{S}_{\rm eff}$, denoted by $\boldsymbol{\zeta}$ in Ref. [28], to lie along $\boldsymbol{e}_Z$. Because of these restrictions, that analysis provides only a parametric solution to $\boldsymbol{r}$. We have, on the other hand, consistently taken into consideration all the leading order spin-orbit interactions and obtained a parametric solution to the entire binary dynamics. In a future communication we will connect the above presented parametric solution to quantities related to observation, especially associated with binary pulsars [45].

In the next section, we will combine the Keplerian-type parametrization developed above with the one presented in Sec. III.

V. THIRD POST-NEWTONIAN ACCURATE GENERALIZED QUASI-KEPLERIAN PARAMETRIZATION FOR COMPACT BINARIES IN ECCENTRIC ORBITS WITH THE FIRST-ORDER SPIN-ORBIT INTERACTION

We are now in a position to have *parametric solution to the dynamics,* defined by the Hamiltonian H, as given by Eq. (2.2). This is done by combining consistently the parametrizations presented in the previous two sections, Secs. III and IV. The two parametric solutions of Secs. III and IV can be added linearly to obtain the PN accurate binary dynamics, given by Eqs. (2.2) and (2.3), for the following reasons. Recall that in the Hamiltonian, given by Eqs. (2.2) and (2.3), the spin-orbit contribution is added linearly to the PN accurate nonspinning contributions. Moreover, as we are considering only leading order spin-orbit interactions, spin-orbit contributions cross only with the Newtonian terms in the Hamiltonian. This is why we can treat the spin-orbit contributions and the nonspinning PN contributions separately and later add the two parametric solutions linearly. However, as a cautionary note, we state that care should be taken while merging the above two parametric solutions to avoid adding similar contributions twice. Finally, we display below, in its entirety, the parametric solution to the conservative third post-Newtonian dynamics of spinning compact binaries moving in an eccentric orbit, in ADM-type coordinates, with spin effects restricted to the leading order spin-orbit interactions:

$$\boldsymbol{r} = r\cos\varphi\boldsymbol{i} + r\sin\varphi\boldsymbol{j}, \tag{5.1}$$

$$\boldsymbol{L} = L\boldsymbol{k}, \tag{5.2}$$

$$\boldsymbol{S} = J\boldsymbol{e}_Z - L\boldsymbol{k}, \tag{5.3}$$

where the basic vectors $(\boldsymbol{i}, \boldsymbol{j}, \boldsymbol{k})$ are explicitly given by

$$\boldsymbol{i} = \cos\Upsilon\boldsymbol{e}_X + \sin\Upsilon\boldsymbol{e}_Y, \tag{5.4a}$$

$$\boldsymbol{j} = -\cos\Theta\sin\Upsilon\boldsymbol{e}_X + \cos\Theta\cos\Upsilon\boldsymbol{e}_Y + \sin\Theta\boldsymbol{e}_Z, \tag{5.4b}$$

$$\boldsymbol{k} = \sin\Theta\sin\Upsilon\boldsymbol{e}_X - \sin\Theta\cos\Upsilon\boldsymbol{e}_Y + \cos\Theta\boldsymbol{e}_Z, \tag{5.4c}$$

and

$$r = a_r(1 - e_r\cos u), \tag{5.5a}$$

$$l \equiv n(t - t_0) = u - e_t\sin u + \left(\frac{g_{4t}}{c^4} + \frac{g_{6t}}{c^6}\right)(v - u) + \left(\frac{f_{4t}}{c^4} + \frac{f_{6t}}{c^6}\right)\sin v + \frac{i_{6t}}{c^6}\sin 2v + \frac{h_{6t}}{c^6}\sin 3v, \tag{5.5b}$$

$$\varphi - \varphi_0 = (1 + k)v + \left(\frac{f_{4\varphi}}{c^4} + \frac{f_{6\varphi}}{c^6}\right)\sin 2v + \left(\frac{g_{4\varphi}}{c^4} + \frac{g_{6\varphi}}{c^6}\right)\sin 3v + \frac{i_{6\varphi}}{c^6}\sin 4v + \frac{h_{6\varphi}}{c^6}\sin 5v, \tag{5.5c}$$

$$\Upsilon - \Upsilon_0 = \frac{\chi_{\rm so}J}{c^2L^3}(v + e\sin v), \tag{5.5d}$$

$$\text{where}\quad v = 2\arctan\left[\left(\frac{1 + e_\varphi}{1 - e_\varphi}\right)^{1/2}\tan\frac{u}{2}\right]. \tag{5.5e}$$

The post-Newtonian accurate expressions for the orbital elements a_r, e_r^2, n, e_t^2, k, and e_φ^2 and the post-Newtonian orbital functions g_{4t}, g_{6t}, f_{4t}, f_{6t}, i_{6t}, h_{6t}, $f_{4\varphi}$, $f_{6\varphi}$, $g_{4\varphi}$, $g_{6\varphi}$, $i_{6\varphi}$, and $h_{6\varphi}$, in terms of E, L, S, η, and α, read

$$\begin{aligned} a_r = \frac{1}{(-2E)}\bigg\{&1 + \frac{(-2E)}{4c^2}\left(-7 + \eta + 4\chi_{\rm so}\cos\alpha\frac{S}{L}\right) + \frac{(-2E)^2}{16c^4}\left[1 + 10\eta + \eta^2 + \frac{1}{(-2EL^2)}(-68 + 44\eta)\right] \\ &+ \frac{(-2E)^3}{192c^6}\bigg[3 - 9\eta - 6\eta^2 + 3\eta^3 + \frac{1}{(-2EL^2)}(864 - 3\pi^2\eta - 2212\eta + 432\eta^2) + \frac{1}{(-2EL^2)^2}(-6432 + 13488\eta \\ &- 240\pi^2\eta - 768\eta^2)\bigg]\bigg\}, \end{aligned} \tag{5.6a}$$

$$\begin{aligned} e_r^2 = 1 + 2EL^2 &+ \frac{(-2E)}{4c^2}\left\{24 - 4\eta - 5(3 - \eta)(-2EL^2) - 16(1 + EL^2)\chi_{\rm so}\cos\alpha\frac{S}{L}\right\} + \frac{(-2E)^2}{8c^4}\bigg\{52 + 2\eta + 2\eta^2 \\ &- (80 - 55\eta + 4\eta^2)(-2EL^2) + \frac{8}{(-2EL^2)}(17 - 11\eta)\bigg\} + \frac{(-2E)^3}{192c^6}\bigg\{-768 - 6\pi^2\eta - 344\eta - 216\eta^2 \\ &+ 3(-2EL^2)(-1488 + 1556\eta - 319\eta^2 + 4\eta^3) - \frac{4}{(-2EL^2)}(588 - 8212\eta + 177\pi^2\eta + 480\eta^2) \\ &+ \frac{192}{(-2EL^2)^2}(134 - 281\eta + 5\pi^2\eta + 16\eta^2)\bigg\}, \end{aligned} \tag{5.6b}$$

$$\begin{aligned} n = (-2E)^{3/2}\bigg\{&1 + \frac{(-2E)}{8c^2}(-15 + \eta) + \frac{(-2E)^2}{128c^4}\left[555 + 30\eta + 11\eta^2 - \frac{192}{\sqrt{-2EL^2}}(5 - 2\eta)\right] \\ &+ \frac{(-2E)^3}{3072c^6}\bigg[-29385 - 4995\eta - 315\eta^2 + 135\eta^3 - \frac{16}{(-2EL^2)^{3/2}}(10080 + 123\pi^2\eta - 13952\eta + 1440\eta^2) \\ &+ \frac{5760}{\sqrt{-2EL^2}}(17 - 9\eta + 2\eta^2)\bigg]\bigg\}, \end{aligned} \tag{5.6c}$$

$$e_t^2 = 1 + 2EL^2 + \frac{-2E}{4c^2}\left\{-8 + 8\eta + (17 - 7\eta)(-2EL^2) - 8\chi_{\rm so}\cos\alpha\frac{S}{L}\right\} + \frac{(-2E)^2}{8c^4}\left\{8 + 4\eta + 20\eta^2 - (-2EL^2)(112 - 47\eta + 16\eta^2) + 24\sqrt{-2EL^2}(5 - 2\eta) + \frac{4}{(-2EL^2)}(17 - 11\eta) - \frac{24}{\sqrt{-2EL^2}}(5 - 2\eta)\right\} + \frac{(-2E)^3}{192c^6}\left\{24(-2 + 5\eta)(-23 + 10\eta + 4\eta^2) - 15(-528 + 200\eta - 77\eta^2 + 24\eta^3)(-2EL^2) - 72(265 - 193\eta + 46\eta^2)\sqrt{-2EL^2} - \frac{2}{(-2EL^2)}(6732 + 117\pi^2\eta - 12508\eta + 2004\eta^2) + \frac{2}{\sqrt{-2EL^2}}(16380 - 19964\eta + 123\pi^2\eta + 3240\eta^2) - \frac{2}{(-2EL^2)^{3/2}}(10080 + 123\pi^2\eta - 13952\eta + 1440\eta^2) + \frac{96}{(-2EL^2)^2}(134 - 281\eta + 5\pi^2\eta + 16\eta^2)\right\}, \tag{5.6d}$$

$$g_{4t} = \frac{3(-2E)^2}{2}\frac{5 - 2\eta}{\sqrt{-2EL^2}}, \tag{5.6e}$$

$$g_{6t} = \frac{(-2E)^3}{192}\left\{\frac{1}{(-2EL^2)^{3/2}}(10080 + 123\pi^2\eta - 13952\eta + 1440\eta^2) + \frac{1}{\sqrt{-2EL^2}}(-3420 + 1980\eta - 648\eta^2)\right\}, \tag{5.6f}$$

$$f_{4t} = -\frac{1}{8}\frac{(-2E)^2}{\sqrt{-2EL^2}}(4 + \eta)\eta\sqrt{1 + 2EL^2}, \tag{5.6g}$$

$$f_{6t} = \frac{(-2E)^3}{192}\frac{1}{\sqrt{1 + 2EL^2}}\left\{\frac{1}{(-2EL^2)^{3/2}}(1728 - 4148\eta + 3\pi^2\eta + 600\eta^2 + 33\eta^3) + 3\sqrt{-2EL^2}\eta(-64 - 4\eta + 23\eta^2) + \frac{1}{\sqrt{-2EL^2}}(-1728 + 4232\eta - 3\pi^2\eta - 627\eta^2 - 105\eta^3)\right\}, \tag{5.6h}$$

$$i_{6t} = \frac{(-2E)^3}{32}\frac{(1 + 2EL^2)}{(-2EL^2)^{3/2}}\eta(23 + 12\eta + 6\eta^2), \tag{5.6i}$$

$$h_{6t} = \frac{13(-2E)^3}{192}\eta^3\left(\frac{1 + 2EL^2}{-2EL^2}\right)^{3/2}, \tag{5.6j}$$

$$k = \frac{3}{c^2L^2}\left\{1 + \frac{\chi_{\rm so}}{3} - \chi_{\rm so}\cos\alpha\frac{S}{L} + \frac{(-2E)}{4c^2}\left(-5 + 2\eta + \frac{35 - 10\eta}{-2EL^2}\right) + \frac{(-2E)^2}{384c^4}\left[120 - 120\eta + 96\eta^2 + \frac{1}{(-2EL^2)}(-10080 + 13952\eta - 123\pi^2\eta - 1440\eta^2) + \frac{1}{(-2EL^2)^2}(36960 - 40000\eta + 615\pi^2\eta + 1680\eta^2)\right]\right\}, \tag{5.6k}$$

$$f_{4\varphi} = \frac{(-2E)^2}{8}\frac{(1 + 2EL^2)}{(-2EL^2)^2}\eta(1 - 3\eta), \tag{5.6l}$$

$$f_{6\varphi} = \frac{1}{256}\frac{(-2E)^3}{(-2EL^2)}\left\{-(44 + 160\eta - 96\eta^2)\eta + \frac{1}{(-2EL^2)}(-256 - 49\pi^2\eta + 1096\eta + 624\eta^2 - 80\eta^3) + \frac{1}{(-2EL^2)^2}(256 + 49\pi^2\eta - 980\eta - 672\eta^2 - 40\eta^3)\right\}, \tag{5.6m}$$

$$g_{4\varphi} = -\frac{3(-2E)^2}{32}\frac{\eta^2}{(-2EL^2)^2}(1 + 2EL^2)^{3/2}, \tag{5.6n}$$

$$g_{6\varphi} = \frac{(-2E)^3}{768}\frac{\sqrt{1 + 2EL^2}}{(-2EL^2)}\eta\biggl\{-27\eta + 78\eta^2 - \frac{1}{(-2EL^2)}(220 + 3\pi^2 + 96\eta + 150\eta^2) + \frac{1}{(-2EL^2)^2}(220 + 3\pi^2 - 120\eta + 45\eta^2)\biggr\}, \tag{5.6o}$$

$$i_{6\varphi} = \frac{(-2E)^3}{128}\frac{(1 + 2EL^2)^2}{(-2EL^2)^3}\eta(5 + 28\eta + 10\eta^2), \tag{5.6p}$$

$$h_{6\varphi} = \frac{5(-2E)^3}{256}\frac{\eta^3}{(-2EL^2)^3}(1 + 2EL^2)^{5/2}, \tag{5.6q}$$

$$\begin{aligned} e_\varphi^2 = {}& 1 + 2EL^2 + \frac{(-2E)}{4c^2}\biggl\{24 - (15 - \eta)(-2EL^2) + 8(1 + 2EL^2)\chi_{\rm so} - 8(3 + 4EL^2)\chi_{\rm so}\cos\alpha\frac{S}{L}\biggr\} \\ & + \frac{(-2E)^2}{16c^4}\biggl\{-32 + 176\eta + 18\eta^2 - (-2EL^2)(160 - 30\eta + 3\eta^2) + \frac{1}{(-2EL^2)}(408 - 232\eta - 15\eta^2)\biggr\} \\ & + \frac{(-2E)^3}{384c^6}\biggl\{-16032 + 2764\eta + 3\pi^2\eta + 4536\eta^2 + 234\eta^3 - 36(248 - 80\eta + 13\eta^2 + \eta^3)(-2EL^2) \\ & - \frac{6}{(-2EL^2)}(2456 - 26860\eta + 581\pi^2\eta + 2689\eta^2 + 10\eta^3) + \frac{3}{(-2EL^2)^2}(27776 - 65436\eta + 1325\pi^2\eta \\ & + 3440\eta^2 - 70\eta^3)\biggr\}. \end{aligned} \tag{5.6r}$$

We recall that e, appearing in Eq. (5.5d), is given by the Newtonian contribution to e_r. The three eccentricities e_r, e_t, and e_φ are related to each other by post-Newtonian corrections

$$\begin{aligned} e_t = {}& e_r\biggl\{1 + \frac{(-2E)}{2c^2}\left(-8 + 3\eta + 2\chi_{\rm so}\cos\alpha\frac{S}{L}\right) + \frac{(-2E)^2}{8c^4}\frac{1}{(-2EL^2)}\Bigl[-34 + 22\eta - (60 - 24\eta)\sqrt{-2EL^2} \\ & + (72 - 33\eta + 12\eta^2)(-2EL^2)\Bigr] + \frac{(-2E)^3}{192c^6}\frac{1}{(-2EL^2)^2}\Bigl[-6432 + 13488\eta - 240\eta\pi^2 - 768\eta^2 \\ & + (-10080 + 13952\eta - 123\eta\pi^2 - 1440\eta^2)\sqrt{-2EL^2} + (2700 - 4420\eta - 3\eta\pi^2 + 1092\eta^2)(-2EL^2) \\ & + (9180 - 6444\eta + 1512\eta^2)(-2EL^2)^{3/2} + (-3840 + 1284\eta - 672\eta^2 + 240\eta^3)(-2EL^2)^2\Bigr]\biggr\}, \end{aligned} \tag{5.7a}$$

$$\begin{aligned} e_\varphi = {}& e_r\biggl\{1 + \frac{(-2E)}{2c^2}\left(\eta + 2\chi_{\rm so} - 2\chi_{\rm so}\cos\alpha\frac{S}{L}\right) + \frac{(-2E)^2}{32c^4}\frac{1}{(-2EL^2)}[136 - 56\eta - 15\eta^2 + \eta(20 + 11\eta)(-2EL^2)] \\ & + \frac{(-2E)^3}{768c^6}\frac{1}{(-2EL^2)^2}[31872 - 88404\eta + 2055\eta\pi^2 + 4176\eta^2 - 210\eta^3 + (2256 + 10228\eta - 15\eta\pi^2 \\ & - 2406\eta^2 - 450\eta^3)(-2EL^2) + 6\eta(136 + 34\eta + 31\eta^2)(-2EL^2)^2]\biggr\}, \end{aligned} \tag{5.7b}$$

and hence it is possible to describe the binary dynamics in terms of one of the eccentricities.

We emphasize that, while adapting the parametrization to describe the binary dynamics, care should be taken to restrict orbital elements to the required post-Newtonian order.

As noted earlier, Θ, the precessional angle for $\boldsymbol{k}$, is given by

$$\sin\Theta = \frac{S\sin\alpha}{J}, \tag{5.8a}$$

$$\cos\Theta = \frac{L + S\cos\alpha}{J}, \tag{5.8b}$$

where the magnitude of the total angular momentum is given by $J = (L^2 + S^2 + 2LS\cos\alpha)^{1/2}$.

Finally, we emphasize that the parametric solution, given by Eqs. (5.1), (5.2), (5.3), (5.4), (5.5), (5.6), (5.7), and (5.8), describes the entire conservative post-Newtonian accurate dynamics of a spinning compact binary in an eccentric orbit when the spin effects are restricted to the leading order spin-orbit interaction. This means the parametrization consistently describes not only the precessional motion of the orbit inside the orbital plane but also the precessional motions of the orbital plane and the spins themselves.

It is possible, though tedious, to show that the combined parametric solution, given by Eqs. (5.1), (5.2), (5.3), (5.4), (5.5), (5.6), (5.7), and (5.8), is indeed a parametric solution to the total orbital dynamics prescribed by Eqs. (2.2) and (2.3). To show that, we have computed, using the combined parametric solution, PN accurate expressions for $\dot{r}$, $\dot{\theta}$, and $\dot{\phi}$ in terms of E, L, $\boldsymbol{L}\cdot\boldsymbol{S}_{\rm eff}$, and r with the help of Eqs. (4.27) and (4.28). These expressions were found to be in total agreement with PN accurate expressions for $\dot{r}$, $\dot{\theta}$, and $\dot{\phi}$ computed from the total (reduced) Hamiltonian, given by Eqs. (2.2) and (2.3), using Hamilton's equations of motion [see Eqs. (4.7), (4.8), (4.9), (4.10), and (4.11) and the related discussions].

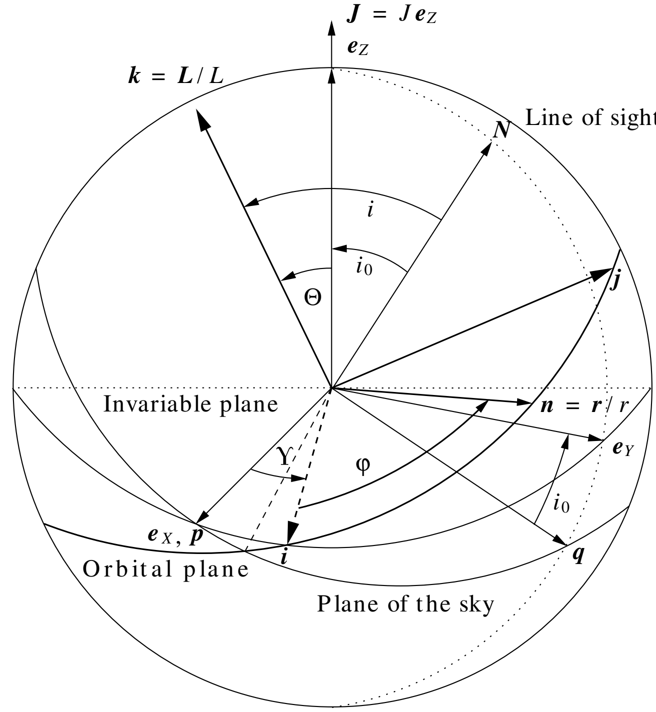

FIG. 2. The convention we adopted to link the orbital frame $(\boldsymbol{i}, \boldsymbol{j}, \boldsymbol{k})$, the invariable frame $(\boldsymbol{e}_X, \boldsymbol{e}_Y, \boldsymbol{e}_Z)$, and the frame $(\boldsymbol{p}, \boldsymbol{q}, \boldsymbol{N})$ associated with the observer. Since we choose the line-of-sight unit vector $\boldsymbol{N}$ to lie in the $\boldsymbol{e}_Y$-$\boldsymbol{e}_Z$ plane, we may align the polarization vector $\boldsymbol{p}$ along $\boldsymbol{e}_X$, where the plane of the sky meets the invariable plane. This implies that $\boldsymbol{q}$ also lies in the $\boldsymbol{e}_Y$-$\boldsymbol{e}_Z$ plane. Therefore, the frames $(\boldsymbol{p}, \boldsymbol{q}, \boldsymbol{N})$ and $(\boldsymbol{e}_X, \boldsymbol{e}_Y, \boldsymbol{e}_Z)$ are connected by a constant angle i_0, which is the constant inclination angle between $\boldsymbol{N}$ and $\boldsymbol{J}$. The polarization vectors $\boldsymbol{p}$ and $\boldsymbol{q}$ span the plane of the sky. The inclination of this plane with respect to the orbital plane is the *orbital* inclination i. The inclination of the orbital plane with respect to the invariable plane is denoted by the constant angle Θ.

VI. THE LEADING PART OF THE QUADRUPOLAR GRAVITATIONAL-WAVE POLARIZATIONS FOR SPINNING COMPACT BINARIES IN ECCENTRIC ORBITS

As an application of the above parametrization, we obtain, for the first time, explicit expressions for h_+ and $h_\times$ suitable to describe gravitational radiation from spinning compact binaries moving in eccentric orbits, corresponding to the cases considered in Sec. IV. The gravitational-wave polarization states, h_+ and $h_\times$, are usually given by

$$h_+ = \frac{1}{2}(p_i p_j - q_i q_j)h_{ij}^{\rm TT}, \tag{6.1a}$$

$$h_\times = \frac{1}{2}(p_i q_j + p_j q_i)h_{ij}^{\rm TT}, \tag{6.1b}$$

where $\boldsymbol{p}$ and $\boldsymbol{q}$ are two orthogonal unit vectors in the plane of the sky, i.e., a plane transverse to the radial direction $\boldsymbol{N}$ (the line of sight), linking the observer to the source (see Fig. 2).

The TT part of the radiation field, $h_{ij}^{\rm TT}$, which depends on the dynamics of the compact binary, is expressible in terms of a post-Newtonian expansion in (v/c). Symbolically, the TT radiation field may be written as

$$h_{ij}^{\rm TT} = \frac{1}{c^4}h_{ij}^{(0)} + \frac{1}{c^5}h_{ij}^{(1)} + \frac{1}{c^6}h_{ij}^{(2)} + \frac{1}{c^7}h_{ij}^{(3)} + \cdots. \tag{6.2}$$

In this paper, for simplicity, we will restrict $h_{ij}^{\rm TT}$ to its leading "quadrupolar" order, namely, to $h_{ij}^{(0)}/c^4$, and denote it by $h_{ij}^{\rm TT}|_{\rm Q}$. However, higher PN corrections to $h_{ij}^{\rm TT}$ are available in the literature. The 2PN corrections to $h_{ij}^{\rm TT}$ for compact binaries moving in general orbits are given in Refs. [25,46]. The spin-orbit and spin-spin interactions directly contribute to $h_{ij}^{\rm TT}$ and were computed in Ref. [23]. For compact binaries, in circular orbits, the explicit expressions for 2.5PN accurate $h_{ij}^{\rm TT}$—corrections that include $h_{ij}^{(5)}/c^9$ in harmonic coordinates—were recently derived in Ref. [5]. We recall that post-Newtonian corrections to $h_{ij}^{\rm TT}$ are usually given in harmonic coordinates, which differ from the one we employed here at 2PN and 3PN orders. However, using coordinate transformations that link harmonic and ADM-type coordinates, given in Ref. [12], it is possible to obtain post-Newtonian corrections to the amplitudes of h_+ and $h_\times$ in ADM-type coordinates.

The explicit expression for $h_{ij}^{\rm TT}$, in the leading part of the quadrupolar approximation, reads

$$h_{km}^{\rm TT}|_{\rm Q} = \frac{4G\mu}{c^4 R'} \mathcal{P}_{ijkm}(\boldsymbol{N})\left(v_{ij} - \frac{GM}{r} n_{ij}\right), \tag{6.3}$$

where $\mathcal{P}_{ijkm}(\boldsymbol{N})$ is the usual transverse-traceless projection operator projecting vectors normal to $\boldsymbol{N}$, where $\boldsymbol{N} = \boldsymbol{R}'/R'$ is the line-of-sight unit vector from the observer to the binary, and $R' = |\boldsymbol{R}'|$ is the corresponding radial distance. We also used $v_{ij} := v_i v_j$ and $n_{ij} := n_i n_j$, where v_i and n_i are the components of the velocity vector $\boldsymbol{v} = d\boldsymbol{r}/dt$ and the unit relative separation vector $\boldsymbol{n} = \boldsymbol{r}/r$, where $r = |\boldsymbol{r}|$.

Using Eqs. (6.1) and (6.3), we obtain $h_+|_{\rm Q}$ and $h_\times|_{\rm Q}$, the expressions for gravitational-wave polarizations when their amplitudes are restricted to the leading quadrupolar order, for compact binaries moving in general orbits as

$$\begin{aligned} h_+|_{\rm Q} &= \frac{2G\mu}{c^4 R'}\left[(p_i p_j - q_i q_j)\left(v_{ij} - \frac{GM}{r} n_{ij}\right)\right] \\ &= \frac{2G\mu}{c^4 R'}\left\{(\boldsymbol{p}\cdot\boldsymbol{v})^2 - (\boldsymbol{q}\cdot\boldsymbol{v})^2 - \frac{GM}{r}[(\boldsymbol{p}\cdot\boldsymbol{n})^2 \right. \\ &\quad \left. - (\boldsymbol{q}\cdot\boldsymbol{n})^2]\right\}, \end{aligned} \tag{6.4a}$$

$$\begin{aligned} h_\times|_{\rm Q} &= \frac{2G\mu}{c^4 R'}\left[(p_i q_j + p_j q_i)\left(v_{ij} - \frac{GM}{r} n_{ij}\right)\right] \\ &= \frac{4G\mu}{c^4 R'}\left[(\boldsymbol{p}\cdot\boldsymbol{v})(\boldsymbol{q}\cdot\boldsymbol{v}) - \frac{GM}{r}(\boldsymbol{p}\cdot\boldsymbol{n})(\boldsymbol{q}\cdot\boldsymbol{n})\right]. \end{aligned} \tag{6.4b}$$

The expressions for $h_+|_{\rm Q}$ and $h_\times|_{\rm Q}$ for spinning compact binaries in eccentric orbits are obtained by adapting the radial separation and velocity vectors, $\boldsymbol{r}$ and $\boldsymbol{v} = d\boldsymbol{r}/dt$, to the orthonormal triad $(\boldsymbol{p}, \boldsymbol{q}, \boldsymbol{N})$. This is easily achieved in the following way. We deduce that the explicit parametric representation for $\boldsymbol{r}$, given by Eqs. (5.1) and (5.4), in terms of the reference triad $(\boldsymbol{e}_X, \boldsymbol{e}_Y, \boldsymbol{e}_Z)$ is given by

$$\begin{aligned} \boldsymbol{r} &= r(\cos\Upsilon\cos\varphi - \cos\Theta\sin\Upsilon\sin\varphi)\boldsymbol{e}_X \\ &\quad + r(\sin\Upsilon\cos\varphi + \cos\Theta\cos\Upsilon\sin\varphi)\boldsymbol{e}_Y \\ &\quad + r\sin\Theta\sin\varphi\boldsymbol{e}_Z. \end{aligned} \tag{6.5}$$

In the above equation, the angles φ and Υ along with r depend on the orbital dynamics. However, Θ is a constant angle—a direct consequence of choosing two distinct cases for the parametrization (see discussion in Sec. IV).

To compute $h_+|_{\rm Q}$ and $h_\times|_{\rm Q}$, one needs to choose a convention for the direction and orientation of the orbit with respect to the plane of sky. In our approach, the orthonormal triad $(\boldsymbol{p}, \boldsymbol{q}, \boldsymbol{N})$ is connected to the reference triad $(\boldsymbol{e}_X, \boldsymbol{e}_Y, \boldsymbol{e}_Z)$ by a constant angle i_0 (see Fig. 2).

In particular, we connect the reference triad $(\boldsymbol{e}_X, \boldsymbol{e}_Y, \boldsymbol{e}_Z)$ to the observer triad $(\boldsymbol{p}, \boldsymbol{q}, \boldsymbol{N})$ by a rotation around $\boldsymbol{p}$ via a constant angle i_0

$$\begin{pmatrix} \boldsymbol{e}_X \\ \boldsymbol{e}_Y \\ \boldsymbol{e}_Z \end{pmatrix} = \begin{pmatrix} 1 & 0 & 0 \\ 0 & C_{i_0} & S_{i_0} \\ 0 & -S_{i_0} & C_{i_0} \end{pmatrix}\begin{pmatrix} \boldsymbol{p} \\ \boldsymbol{q} \\ \boldsymbol{N} \end{pmatrix}, \tag{6.6}$$

where C_{i_0} and S_{i_0} are shorthand notations for $\cos i_0$ and $\sin i_0$. It is now straightforward to get the explicit expressions for the radial separation and velocity vectors in terms of the orbital triad $(\boldsymbol{p}, \boldsymbol{q}, \boldsymbol{N})$ associated with the observer. The vectorial equation for $\boldsymbol{r}$ reads

$$\begin{aligned} \boldsymbol{r} &= r(\cos\Upsilon\cos\varphi - C_\Theta\sin\Upsilon\sin\varphi)\boldsymbol{p} \\ &\quad + r[C_{i_0}\sin\Upsilon\cos\varphi - (S_{i_0}S_\Theta - C_{i_0}C_\Theta\cos\Upsilon)\sin\varphi]\boldsymbol{q} \\ &\quad + r[S_{i_0}\sin\Upsilon\cos\varphi + (C_{i_0}S_\Theta + S_{i_0}C_\Theta\cos\Upsilon)\sin\varphi]\boldsymbol{N}, \end{aligned} \tag{6.7}$$

where C_Θ and S_Θ are shorthand notations for $\cos\Theta$ and $\sin\Theta$. The radial velocity vector $\boldsymbol{v} = d\boldsymbol{r}/dt$ is given by

$$\begin{aligned} \boldsymbol{v} &= \{[-C_\Theta\dot{r}\sin\Upsilon - r(\dot\varphi + C_\Theta\dot\Upsilon)\cos\Upsilon]\sin\varphi + [-r(C_\Theta\dot\varphi + \dot\Upsilon)\sin\Upsilon + \dot{r}\cos\Upsilon]\cos\varphi\}\boldsymbol{p} + \{[-rC_{i_0}(\dot\varphi + C_\Theta\dot\Upsilon)\sin\Upsilon \\ &\quad + C_{i_0}C_\Theta\dot{r}\cos\Upsilon - S_{i_0}S_\Theta\dot{r}]\sin\varphi + [C_{i_0}\dot{r}\sin\Upsilon + rC_{i_0}(C_\Theta\dot\varphi + \dot\Upsilon)\cos\Upsilon - S_{i_0}S_\Theta r\dot\varphi]\cos\varphi\}\boldsymbol{q} \\ &\quad + \{[-rS_{i_0}(\dot\varphi + C_\Theta\dot\Upsilon)\sin\Upsilon + S_{i_0}C_\Theta\dot{r}\cos\Upsilon + C_{i_0}S_\Theta\dot{r}]\sin\varphi + [S_{i_0}\dot{r}\sin\Upsilon + rS_{i_0}(C_\Theta\dot\varphi + \dot\Upsilon)\cos\Upsilon \\ &\quad + C_{i_0}S_\Theta r\dot\varphi]\cos\varphi\}\boldsymbol{N}. \end{aligned} \tag{6.8}$$

Note that, while computing $\boldsymbol{v}$, we have kept Θ and i_0 as constant angles. We point out that the way we defined the angle i_0 is similar to the manner in which the "inclination" was defined in Ref. [47] and Ref. [23] [see, e.g., discussions prior to Eqs. (4.23) in subsection C under Sec. IV in Ref. [23]].

It is now straightforward, though lengthy, to obtain the explicit expressions for gravitational-wave polarizations for spinning compact binaries moving in eccentric orbits when the dynamics includes the leading spin-orbit interaction. The expressions $h_+|_{\rm Q}$ and $h_\times|_{\rm Q}$, giving the gravitational-wave polarizations with amplitudes due to the quadrupolar contributions, read

$$h_+|_Q = \frac{2G\mu}{c^4R'}\bigg(\bigg\{-S_{i_0}C_{i_0}S_\Theta\bigg(\frac{GM}{r} - \dot{r}^2 + r^2\dot{\varphi}^2 + C_\Theta r^2\dot{\varphi}\,\dot{\Upsilon}\bigg)\sin\Upsilon + S_{i_0}C_{i_0}S_\Theta r\dot{r}(2C_\Theta\dot{\varphi} + \dot{\Upsilon})\cos\Upsilon + \frac{1}{2}(1 + C_{i_0}^2) \times\bigg[C_\Theta\bigg(\frac{GM}{r} - \dot{r}^2 + r^2\dot{\varphi}^2 + r^2\dot{\Upsilon}^2\bigg) + (1 + C_\Theta^2)r^2\dot{\varphi}\,\dot{\Upsilon}\bigg]\sin2\Upsilon - \frac{1}{2}(1 + C_{i_0}^2)r\dot{r}[(1 + C_\Theta^2)\dot{\varphi} + 2C_\Theta\dot{\Upsilon}]\cos2\Upsilon - \frac{3}{2}S_{i_0}^2S_\Theta^2r\dot{r}\,\dot{\varphi}\bigg\}\sin2\varphi + \bigg\{S_{i_0}C_{i_0}S_\Theta r\dot{r}(2\dot{\varphi} + C_\Theta\dot{\Upsilon})\sin\Upsilon + S_{i_0}C_{i_0}S_\Theta\bigg[r^2\dot{\varphi}\,\dot{\Upsilon} + C_\Theta\bigg(\frac{GM}{r} - \dot{r}^2 + r^2\dot{\varphi}^2\bigg)\bigg]\cos\Upsilon - \frac{1}{2}(1 + C_{i_0}^2)r\dot{r}[2C_\Theta\dot{\varphi} + (1 + C_\Theta^2)\dot{\Upsilon}]\sin2\Upsilon - \frac{1}{4}(1 + C_{i_0}^2)\bigg[4C_\Theta r^2\dot{\varphi}\,\dot{\Upsilon} + (1 + C_\Theta^2)\times\bigg(\frac{GM}{r} - \dot{r}^2 + r^2\dot{\varphi}^2 + r^2\dot{\Upsilon}^2\bigg)\bigg]\cos2\Upsilon - \frac{3}{4}S_{i_0}^2S_\Theta^2\bigg(\frac{GM}{r} - \dot{r}^2 + r^2\dot{\varphi}^2 - \frac{1}{3}r^2\dot{\Upsilon}^2\bigg)\bigg\}\cos2\varphi - S_{i_0}C_{i_0}S_\Theta C_\Theta r\dot{r}\,\dot{\Upsilon}\sin\Upsilon + S_{i_0}C_{i_0}S_\Theta\bigg[r^2\dot{\varphi}\,\dot{\Upsilon} - C_\Theta\bigg(\frac{GM}{r} - \dot{r}^2 - r^2\dot{\varphi}^2\bigg)\bigg]\cos\Upsilon - \frac{1}{2}(1 + C_{i_0}^2)S_\Theta^2r\dot{r}\,\dot{\Upsilon}\sin2\Upsilon - \frac{1}{4}(1 + C_{i_0}^2)S_\Theta^2\bigg(\frac{GM}{r} - \dot{r}^2 - r^2\dot{\varphi}^2 + r^2\dot{\Upsilon}^2\bigg)\cos2\Upsilon + \frac{1}{4}S_{i_0}^2\bigg[4C_\Theta r^2\dot{\varphi}\,\dot{\Upsilon} + (1 + C_\Theta^2)r^2\dot{\Upsilon}^2 + (1 - 3C_\Theta^2)\bigg(\frac{GM}{r} - \dot{r}^2 - r^2\dot{\varphi}^2\bigg)\bigg]\bigg), \tag{6.9a}$$

$$h_\times|_Q = \frac{2G\mu}{c^4R'}\bigg(\bigg\{S_{i_0}S_\Theta r\dot{r}(2C_\Theta\dot{\varphi} + \dot{\Upsilon})\sin\Upsilon + S_{i_0}S_\Theta\bigg(\frac{GM}{r} - \dot{r}^2 + r^2\dot{\varphi}^2 + C_\Theta r^2\dot{\varphi}\,\dot{\Upsilon}\bigg)\cos\Upsilon - C_{i_0}r\dot{r}[(1 + C_\Theta^2)\dot{\varphi} + 2C_\Theta\dot{\Upsilon}]\sin2\Upsilon - C_{i_0}\bigg[C_\Theta\bigg(\frac{GM}{r} - \dot{r}^2 + r^2\dot{\varphi}^2 + r^2\dot{\Upsilon}^2\bigg) + (1 + C_\Theta^2)r^2\dot{\varphi}\,\dot{\Upsilon}\bigg]\cos2\Upsilon\bigg\}\sin2\varphi + \bigg\{S_{i_0}S_\Theta\bigg[r^2\dot{\varphi}\,\dot{\Upsilon} + C_\Theta\bigg(\frac{GM}{r} - \dot{r}^2 + r^2\dot{\varphi}^2\bigg)\bigg]\sin\Upsilon - S_{i_0}S_\Theta r\dot{r}(2\dot{\varphi} + C_\Theta\dot{\Upsilon})\cos\Upsilon - \frac{1}{2}C_{i_0}\bigg[4C_\Theta r^2\dot{\varphi}\,\dot{\Upsilon} + (1 + C_\Theta^2)\bigg(\frac{GM}{r} - \dot{r}^2 + r^2\dot{\varphi}^2 + r^2\dot{\Upsilon}^2\bigg)\bigg]\sin2\Upsilon + C_{i_0}r\dot{r}[2C_\Theta\dot{\varphi} + (1 + C_\Theta^2)\dot{\Upsilon}]\cos2\Upsilon\bigg\}\cos2\varphi + S_{i_0}S_\Theta\bigg[r^2\dot{\varphi}\,\dot{\Upsilon} - C_\Theta\bigg(\frac{GM}{r} - \dot{r}^2 - r^2\dot{\varphi}^2\bigg)\bigg]\sin\Upsilon + S_{i_0}S_\Theta C_\Theta r\dot{r}\,\dot{\Upsilon}\cos\Upsilon - \frac{1}{2}C_{i_0}S_\Theta^2\bigg(\frac{GM}{r} - \dot{r}^2 - r^2\dot{\varphi}^2 + r^2\dot{\Upsilon}^2\bigg)\sin2\Upsilon + C_{i_0}S_\Theta^2r\dot{r}\,\dot{\Upsilon}\cos2\Upsilon\bigg). \tag{6.9b}$$

We again remind the reader that the orbital phase is denoted by φ, the angle Υ describes the phase of the line of nodes $\boldsymbol{i}$, $\dot{\varphi} = d\varphi/dt$, $\dot{\Upsilon} = d\Upsilon/dt$, and $\dot{r} = (\boldsymbol{n}\cdot\boldsymbol{v})$. The parametric PN accurate expressions for these time derivatives can easily be computed using the parametric solution as $\dot{r} = dr/dt = (dr/du)(du/dt)$, $\dot{\varphi} = d\varphi/dt = (d\varphi/dv)(dv/du)(du/dt)$, and $\dot{\Upsilon} = d\Upsilon/dt = (d\Upsilon/dv)\times(dv/du)(du/dt)$.

Notice that the temporally evolving (observational) orbital inclination i (see Fig. 2), defined by $\cos i = \boldsymbol{N}\cdot\boldsymbol{k}$, does not enter the expressions for $h_+|_Q$ and $h_\times|_Q$. However, using i_0, Θ, and Υ, the time evolution of i is simply given by

$$\cos i = \boldsymbol{N}\cdot\boldsymbol{k} = C_{i_0}C_\Theta - S_{i_0}S_\Theta\cos\Upsilon, \tag{6.10a}$$

$$\sin i = |\boldsymbol{N}\times\boldsymbol{k}| = [(S_{i_0}C_\Theta + C_{i_0}S_\Theta\cos\Upsilon)^2 + S_\Theta^2\sin^2\Upsilon]^{1/2} = [1 - (C_{i_0}C_\Theta - S_{i_0}S_\Theta\cos\Upsilon)^2]^{1/2}. \tag{6.10b}$$

The equation for $\cos i$ is in agreement with Eq. (6) in Ref. [47]. We may also obtain a differential equation for the time evolution of i, as given in Ref. [35]. To get that, we differentiate $\cos i = \boldsymbol{N}\cdot\boldsymbol{k}$ with respect to time and make use of $\dot{\boldsymbol{k}} = \dot{\boldsymbol{L}}/L$ with Eqs. (4.2a) and (6.10b). In this way, we deduce the following differential equation for the orbital inclination i:

$$\frac{di}{dt} = \frac{1}{c^2r^3}\boldsymbol{S}_{\rm eff}\cdot\frac{\boldsymbol{N}\times\boldsymbol{k}}{\sin i} = \frac{1}{c^2r^3}\boldsymbol{S}_{\rm eff}\cdot\frac{\boldsymbol{N}\times\boldsymbol{k}}{|\boldsymbol{N}\times\boldsymbol{k}|}, \tag{6.11}$$

which agrees with Eq. (5.15) of Ref. [35].

Equations (6.9) are useful for scenarios where the angle Θ is a constant. This is true for the two cases where our parametric solution is applicable [see discussions in Sec. IV after Eqs. (4.22)].

The approach to compute $h_+|_Q$ and $h_\times|_Q$ may be adapted to include higher order spin effects such as spin-spin interactions. In this case, Θ will no longer be a constant angle, and expressions for the velocity vector $\boldsymbol{v}$ and hence $h_+|_Q$ and $h_\times|_Q$ will also depend on $\dot{\Theta}$.

The nonspinning limit, as given by Eqs. (6) in Ref. [24], is obtained in the following way. We note that when $S \to 0$, $\boldsymbol{J}$ is identical to $\boldsymbol{L}$, which implies $\Theta \to 0$, $\theta \to \pi/2$, and $i_0 \to i$, i being the angle between $\boldsymbol{N}$ and $\boldsymbol{L}$. In this limit, Eqs. (4.27) and (4.28b) indicate that $\Upsilon + \varphi = \phi$ and $\dot{\Upsilon} + \dot{\varphi} = \dot{\phi}$. This leads to Eqs. (6) in Ref. [24] which read

$$h_+|_{\rm Q} = -\frac{G\mu}{c^4R'}\bigg\{(1 + C_i^2)\bigg[2\dot{r}r\dot{\phi}\sin(2\phi) + \bigg(\frac{GM}{r} - \dot{r}^2 + r^2\dot{\phi}^2\bigg)\cos(2\phi)\bigg] + S_i^2\bigg(\frac{GM}{r} - \dot{r}^2 - r^2\dot{\phi}^2\bigg)\bigg\}, \tag{6.12a}$$

$$h_\times|_{\rm Q} = -\frac{2G\mu C_i}{c^4R'}\bigg[\bigg(\frac{GM}{r} - \dot{r}^2 + r^2\dot{\phi}^2\bigg)\sin(2\phi) - 2\dot{r}r\dot{\phi}\cos(2\phi)\bigg], \tag{6.12b}$$

where C_i and S_i are shorthand notations for $\cos i$ and $\sin i$.

The temporal evolution of h_+ and $h_\times$, given by Eqs. (6.9), may be obtained by adapting the "phasing formalism," presented in Ref. [24], and this will be reported soon [48]. However, it should be noted that the parametrization, given by Eqs. (5.1), (5.2), (5.3), (5.4), (5.5), (5.6), (5.7), and (5.8), will be sufficient to determine the 3PN accurate conservative time evolution, which includes the leading order spin-orbit interaction.

VII. CONCLUSIONS

We have presented Keplerian-type parametrization for the solution of post-Newtonian accurate conservative dynamics of spinning compact binaries moving in eccentric orbits. The above PN accurate dynamics consisted of 3PN accurate conservative orbital dynamics, associated with nonspinning compact objects, influenced by the leading order spin-orbit interactions. The orbital elements of the representation were explicitly obtained in terms of the conserved orbital energy, angular momentum, and a quantity that characterizes the leading order spin-orbit interactions in ADM-type coordinates. Our parametric solution is applicable in two distinct cases, namely, case (i), the equal-mass case and case (ii), the single-spin case. We also derived expressions for gravitational-wave polarizations suitable to describe gravitational radiation from spinning compact binaries moving in eccentric orbits.

The present work has several possible applications and some of them are currently under investigation. Employing the phasing formalism given by Ref. [24], along with our parametric solutions and expressions for h_+ and $h_\times$, we will, in the near future, obtain gravitational-wave polarizations suitable to describe gravitational radiation from spinning compact binaries moving in inspiralling eccentric orbits [48]. Our parametric solution for the two cases considered implies that the associated PN accurate conservative binary dynamics will not be chaotic. This is so, as our solution can analytically determine the associated dynamics. It will be interesting to explore (again) numerically the scenarios where our parametrization is valid and investigate if the numerical solutions still predict chaos. Finally, as mentioned earlier, the fully 2PN accurate timing formula may be derived using our parametric solution as a crucial input. This may be required as spin-orbit interactions essentially enter at 2PN order for binary pulsars and their effects leave observational signature [35,49–51].

It is highly desirable to extend the present work in the following directions. In the literature, there exist PN accurate orbital equations of motion for spinning compact binaries where spin-orbit interactions are also PN accurate [22]. It will be interesting to see if a parametric solution is possible for the above dynamics. Naturally, it will be interesting to include spin-spin effects in our parametric solution. However, all these extensions are not straightforward and the parametric solutions for these cases, most probably, will not be as elegant as the one presented in this paper.

ACKNOWLEDGMENTS

We are indebted to Gerhard Schäfer for helpful discussions and encouragement. We gratefully acknowledge the financial support of the Deutsche Forschungsgemeinschaft (DFG) through SFB/TR7 "Gravitationswellenastronomie." The algebraic computations appearing in this paper were performed using MAPLE and MATHEMATICA.

[1] The following URLs provide a wealth of information about the ground- and space-based gravitational-wave interferometers: http://www.ligo.caltech.edu, http://www.virgo.infn.it, http://www.geo600.uni-hannover.de, http://tamago.mtk.nao.ac.jp, and http://lisa.nasa.gov.

[2] L. P. Grishchuk, V. M. Lipunov, K. A. Postnov, M. E. Prokhorov, and B. S. Sathyaprakash, Phys. Usp. **44**, 1 (2001) [Usp. Fiz. Nauk **171**, 3 (2001)].

[3] V. Kalogera *et al.*, Astrophys. J. **601**, L179 (2004).

[4] L. Blanchet, T. Damour, G. Esposito-Farèse, and B. R. Iyer, Phys. Rev. Lett. **93**, 091101 (2004).

[5] K. G. Arun, L. Blanchet, B. R. Iyer, and M. S. S. Qusailah, Classical Quantum Gravity **21**, 3771 (2004).

[6] B. F. Schutz, in *The Detection of Gravitational Waves*, edited by D. G. Blair (Cambridge University, Cambridge, England, 1987), p. 330.

[7] P. Jaranowski and G. Schäfer, Phys. Rev. D **55**, 4712 (1997); **57**, 7274 (1998); **60**, 124003 (1999).

[8] T. Damour, P. Jaranowski, and G. Schäfer, Phys. Rev. D **62**, 021501(R) (2000); **63**, 029903(E) (2001); **63**, 044021 (2001); **66**, 029901(E) (2002).
[9] T. Damour, P. Jaranowski, and G. Schäfer, Phys. Lett. B **513**, 147 (2001).
[10] C. Königsdörffer, G. Faye, and G. Schäfer, Phys. Rev. D **68**, 044004 (2003).
[11] L. Blanchet and G. Faye, Phys. Lett. A **271**, 58 (2000); Phys. Rev. D **63**, 062005 (2000); J. Math. Phys. (N.Y.) **41**, 7675 (2000); **42**, 4391 (2001).
[12] V. C. de Andrade, L. Blanchet, and G. Faye, Classical Quantum Gravity **18**, 753 (2001).
[13] L. Blanchet and B. R. Iyer, Classical Quantum Gravity **20**, 755 (2003).
[14] Y. Itoh and T. Futamase, Phys. Rev. D **68**, 121501 (2003).
[15] Y. Itoh, Phys. Rev. D **69**, 064018 (2004).
[16] L. Blanchet, T. Damour, and G. Esposito-Farèse, Phys. Rev. D **69**, 124007 (2004).
[17] For a brief introduction to spin effects in general relativity, see G. Schäfer, Gen. Relativ. Gravit. **36**, 2223 (2004).
[18] Numerous authors have worked on the dynamics of two spinning bodies of comparable mass. For a classical thorough review, see T. Damour, in *300 Years of Gravitation*, edited by S. Hawking and W. Israel (Cambridge University, Cambridge, England, 1987), p. 128.
[19] T. Damour, Phys. Rev. D **64**, 124013 (2001).
[20] Recent numerical investigations into the PN accurate dynamics of spinning compact binaries are usually motivated by the desire to address the question of chaos in the dynamics of these binaries. See M. D. Hartl and A. Buonanno, gr-qc/0407091 [Phys. Rev. D (to be published)], and references therein.
[21] The data analysis challenge related to the detection of gravitational waves from spinning compact binaries with templates that depend on a minimum number of parameters and which will mimic the actual signal, characterized by large number of orbital and binary parameters, are being addressed by many groups. See A. Buonanno, Y. Chen, Y. Pan, and M. Vallisneri, Phys. Rev. D **70**, 104003 (2004), and references therein.
[22] H. Tagoshi, A. Ohashi, and B. J. Owen, Phys. Rev. D **63**, 044006 (2001).
[23] L. E. Kidder, Phys. Rev. D **52**, 821 (1995).
[24] T. Damour, A. Gopakumar, and B. R. Iyer, Phys. Rev. D **70**, 064028 (2004).
[25] A. Gopakumar and B. R. Iyer, Phys. Rev. D **56**, 7708 (1997).
[26] R.-M. Memmesheimer, A. Gopakumar, and G. Schäfer, Phys. Rev. D **70**, 104011 (2004).
[27] The words ''almost analytic'' or ''semianalytic'' parametrization are used to indicate that we have not yet provided an analytic solution to the PN accurate ''Kepler equation,'' namely, Eq. (5.5b), present in the PN accurate generalized quasi-Keplerian parametrization. This is currently in preparation. M. Haney and A. Gopakumar (to be published).
[28] N. Wex, Classical Quantum Gravity **12**, 983 (1995).
[29] S. Suzuki and K. Maeda, Phys. Rev. D **55**, 4848 (1997).
[30] M. Burgay, *et al.*, Nature (London) **426**, 531 (2003).
[31] T. Damour and J. Taylor, Phys. Rev. D **45**, 1840 (1992).
[32] I. H. Stairs, Living Rev. Relativity **6**, 5 (2003).
[33] T. Damour and N. Deruelle, Ann. Inst. Henri Poincare Phys. Theor. **43**, 107 (1985).
[34] T. Damour and N. Deruelle, Ann. Inst. Henri Poincare Phys. Theor. **44**, 263 (1986).
[35] T. Damour and G. Schäfer, Nuovo Cimento Soc. Ital. Fis., B **101**, 127 (1988).
[36] M. Kramer *et al.*, in *Binary Radio Pulsars*, edited by F. A. Rasio and I. H. Stairs, ASP Conference Series Vol. 328 (Astronomical Society of the Pacific, Provo, UT, 2005).
[37] M. Kramer *et al.*, astro-ph/0409379.
[38] R. Arnowitt, S. Deser, and C. W. Misner, in *Gravitation: An Introduction to Current Research*, edited by L. Witten (Wiley, New York, 1962); gr-qc/0405109.
[39] It turned out that the 3PN accurate Hamiltonian, when it was derived for the first time, involved derivatives of the phase space variables. However, using PN accurate higher order contact transformation, the above Hamiltonian was later reduced to an ordinary Hamiltonian, which depends only on the phase space variables. We refer to the above ordinary Hamiltonian as the 3PN accurate Hamiltonian in ADM-type coordinates.
[40] T. Damour, P. Jaranowski, and G. Schäfer, Phys. Rev. D **62**, 044024 (2000).
[41] M. H. L. Pryce, Proc. R. Soc. London A **195**, 62 (1949).
[42] T. D. Newton and E. P. Wigner, Rev. Mod. Phys. **21**, 400 (1949).
[43] T. Damour and N. Deruelle, Ann. Inst. Henri Poincare Phys. Theor. **43**, 107 (1985).
[44] G. Schäfer and N. Wex, Phys. Lett. A **174**, 196 (1993); **177**, 461(E) (1993).
[45] C. Königsdörffer and A. Gopakumar (to be published).
[46] C. M. Will and A. G. Wiseman, Phys. Rev. D **54**, 4813 (1996).
[47] D. Lai, L. Bildsten, and V. M. Kaspi, Astrophys. J. **452**, 819 (1995).
[48] C. Königsdörffer and A. Gopakumar (to be published).
[49] T. Damour and R. Ruffini, C. R. Hebd. Seances Acad. Sci., Ser. A **279**, 971 (1974).
[50] R. F. O'Connell, Phys. Rev. Lett. **93**, 081103 (2004).
[51] I. H. Stairs, S. E. Thorsett, and Z. Arzoumanian, Phys. Rev. Lett. **93**, 141101 (2004).